RSC Advances

ROYAL SOCIETY OF CHEMISTRY

www.rsc.org/advances

RSC Advances

RSCPublishing

REVIEW ARTICLE

Polarizability as a landmark property for fullerene chemistry and materials science

Cite this: DOI: 10.1039/x0xx00000x

Denis Sh. Sabirov

Received 00th January 2014,
Accepted 00th January 2014

DOI: 10.1039/x0xx00000x

www.rsc.org/

The review summarizes data on dipole polarizability of fullerenes and their derivatives, covering the most widespread classes of fullerene-containing molecules (fullerenes, fullerene exohedral derivatives, fullerene dimers, endofullerenes, fullerene ions, and derivatives with ionic bonds). These are currently presented by experimental and mainly theoretical works. Particular attention is paid to the analysis of the computational data in terms of additive schemes that assists understanding the changes in polarizability upon fullerene functionalization and provides general formula for calcultation of polarizability for certain classes of the exohedral derivatives. Additionally, application of polarizability to physical and chemical problems of fullerene science is discussed. It includes aspects of fullerene reactivity, physicochemical processes in carbon nanostructures (quenching of electronically-excited states, nanocapillarity, *etc.*) as well as use of fullerene adducts as electron-acceptor materials for organic solar cells and molecular switch devices.

1 Introduction

Fullerenes are undoubtedly the tangible embodiment of abstract beauty. Indeed, researchers working in the field of fullerene science usually point out the perfect shapes of their molecules. However, this is not the only reason why fullerenes attract. Due to their chemical structure, fullerenes and their derivatives have unique properties, promising for diverse applications in materials science, pharmaceutics, and nanotechnology. Astounding history of fullerenes discovery started with theoretical prediction of C_{60} by Eiji Ōsawa in 1970,[1] semiempirical calculations of C_{20} and C_{60} by Bochvar and Galpern in 1974,[2] and, finally, experimental detection of this compound by Kroto *et al.* in 1985.[3] Thus, from the beginning, fullerene science has been evolving based on relations between theory and experiment.[4]

Theoretical (mainly quantum-chemical) studies currently retain special place in fullerene science. When the buckminsterfullerene was a low available chemical, its properties used to be calculated.[5] Nowadays, it has become a common compound but not its derivatives or higher/smaller fullerenes. The main difficulty in obtaining pure samples of individual fullerene derivatives deals with non-selectivity of the addition reactions to fullerenes, which is caused by a large number of reactive sites with almost the same reactivity. Therefore, theoretical approaches are developed to preliminarily assess the utility of fullerene derivatives. In this aspect, we should mention computational design of 6.6-closed and 5.6-open $C_{60}CR^1R^2$ adducts with improved electronic properties,[6] fullerene-based compounds with desirable static dielectric constants,[7] polarizability,[8,9] or hyperpolarizability.[10–13] Such approaches allow defining structures of the prospective compounds before the synthetic procedures and focusing on the synthesis of the desired adducts.

Polarizability (or dipole polarizability) of fullerenes and their derivatives seems to be very important among the mentioned properties because it defines many physical and chemical processes: intermolecular interactions, optical properties (*e.g.*, Kerr effect and Rayleigh light scattering), chemical reactions, and many others.[14–16] Thus, it is highly informative and used in the materials design with advanced properties, *e.g.*, photomodulated systems,[17] molecular functional materials with electron-transfer capability,[18] and compounds with enhanced propensity for supramolecular complexes formation.[19]

Studies on fullerene polarizability have started from the first theoretical works of Fowler *et al.*[20] (1990) and Pederson and Quong[21] (1992). Later, French scientific group has performed the first direct measurements (1999).[22] These first works have elucidated that fullerenes are highly polarizable species. It means that analysis of physicochemical processes in fullerene-containing systems should not ignore their polarizability. Currently, the data on the polarizability of diverse fullerenes and their derivatives are presented in periodicals. Experimental studies on C_{60} polarizability and its clusters have been previously partly reviewed[15] as well as DFT studies on the polarizability of C_{60} and C_{70} adducts.[8] However, many

interesting works have remained uncovered. Some of them deal with the relation between the structure and polarizability of fullerene derivatives and its applications to such hot topics of fullerene science as molecular machinery, organic solar cells, and nanomaterials. We think that a review, comprehending these works, should be on time.

The present review is based on two summarizing scientific reports, performed in St. Petersburg (Russia)[23] and Durham (UK),[24] and covers experimental and mainly theoretical works in the field of polarizability of fullerenes and their derivatives from 1990s to 2014. It focuses on the numerical data, coupled with the examples of their application. Note that works on the calculation of fullerene polarizability are numerous, so we have tried to include in the review those, which have not lost the relevance by the moment. Thus, the early estimations (*e.g.*, refs 20, 21, 25–28) are mentioned here without a detailed consideration. The review is chaptered according to the main types of the fullerene-containing systems (fullerenes, fullerene exohedral derivatives, fullerene dimers, endofullerenes, fullerene ions, and derivatives with ionic bonds) and contains the preceding part where we briefly list necessary basic definitions in the field of polarizability. Additionally, it includes a prospective part, devoted to molecular switch, which can exploit polarizability of different exohedral fullerene derivatives.

2 Basic definitions

Polarizability is a molecular property that describes molecule's ability to acquire induced dipole moment in external electric fields.[14,29] When the molecule is under the electric field **E**, its induced dipole moment depends on the dipole polarizability **α** and the high-order polarizabilities (**β**, **γ**, etc.):[30]

$$\boldsymbol{\mu}_{ind} = \boldsymbol{\alpha}\boldsymbol{E} + \tfrac{1}{2}\boldsymbol{\beta}\boldsymbol{E}^2 + \tfrac{1}{6}\boldsymbol{\gamma}\boldsymbol{E}^3 + \ldots \quad (1)$$

In the case of weak fields, $\boldsymbol{\mu}_{ind}$ can be accurately calculated neglecting the high-order terms:

$$\boldsymbol{\mu}_{ind} = \boldsymbol{\alpha}\mathbf{E} \quad (2)$$

where **α** is polarizability tensor in arbitrary coordinate system (*X*, *Y*, *Z*):

$$\boldsymbol{\alpha} = \begin{pmatrix} \alpha_{XX} & \alpha_{XY} & \alpha_{XZ} \\ \alpha_{YX} & \alpha_{YY} & \alpha_{YZ} \\ \alpha_{ZX} & \alpha_{ZY} & \alpha_{ZZ} \end{pmatrix}, \quad (3)$$

which is symmetric about the main diagonal $\alpha_{ij} = \alpha_{ji}$. It can be considered in the eigen coordinate system (*x*, *y*, *z*) when all the non-diagonal elements become zero:

$$\boldsymbol{\alpha} = \begin{pmatrix} \alpha_{xx} & 0 & 0 \\ 0 & \alpha_{yy} & 0 \\ 0 & 0 & \alpha_{zz} \end{pmatrix}, \quad (4)$$

In classic theory, the values α_{xx}, α_{yy}, and α_{zz} are interpreted as main semiaxes of polarizability ellipsoid of the molecule.[29] These are also used for calculation of mean polarizability α and anisotropy of polarizability a^2:

$$\alpha = \frac{1}{3}\left(\alpha_{xx} + \alpha_{yy} + \alpha_{zz}\right) \quad (5)$$

$$a^2 = \frac{1}{2}\left(\left(\alpha_{xx} - \alpha_{yy}\right)^2 + \left(\alpha_{xx} - \alpha_{zz}\right)^2 + \left(\alpha_{yy} - \alpha_{zz}\right)^2\right) \quad (6)$$

These two properties are measurable.[14,29] The trace of tensor **α** is invariant under coordinate system:

$$\alpha_{xx} + \alpha_{yy} + \alpha_{zz} = \alpha_{XX} + \alpha_{YY} + \alpha_{ZZ}, \quad (7)$$

so the diagonal elements of the non-diagonalized tensor (3) are also suitable for calculation of mean polarizability by eqn (5). If the elements from the non-diagonalized tensor are used for calculation of the anisotropy, formula (6) obtains the additional terms:[29]

$$a^2 = \frac{1}{2}[\left(\alpha_{XX} - \alpha_{YY}\right)^2 + \left(\alpha_{XX} - \alpha_{ZZ}\right)^2 + \left(\alpha_{YY} - \alpha_{ZZ}\right)^2 + 6\left(\alpha_{XY}^2 + \alpha_{XZ}^2 + \alpha_{YZ}^2\right)] \quad (8)$$

Polarizability has the dimension of volume (and expressed in Å^3 or atomic units; 1 a.u. = 0.148 Å^3) that can be interpreted as a degree of the filling the space by the molecule's electronic cloud. Therefore, molecular systems with a large number of electrons should demonstrate high α values.[29]

The discussed polarizability is related to the static case of electronic cloud polarization and so-called static electronic polarizability. In the dynamic case, frequency-dependent polarizability α(ω) is considered. Its relation with the static value is roughly described by the following equation:[29]

$$\alpha(\omega) = \alpha\frac{\omega_0^2}{\omega_0^2 - \omega^2}, \quad (9)$$

where frequency ω_0 characterizes the binding of electrons in the molecule.

Electronic polarizability is directly deducible from experiments if we deal with nonpolar substances. In polar cases, orientational polarizability should be taken into account. The last one depends on the permanent dipole moment of the molecule μ_0 and temperature:

$$\alpha_{or} = \frac{\mu_0^2}{3kT} \quad (10)$$

Molecular beam deflection[15] and interferometry[31,32] seem to be the main experimental techniques for determination of polarizability and its anisotropy. These methods require

significant amounts of substances that is usually impossible in the case of fullerene derivatives, which, in addition, have propensity for dissociation (especially, when irradiated). Two reasons above impose limitations on application of the mentioned experimental techniques to fullerene derivatives. The solution of this problem has come from the computational techniques (mainly, quantum-chemical methods). Currently, there are many approaches that can be applied to calculation of polarizability of diverse carbon nanostructures. These are based on additivity, dipole interaction, linear response theory, or finite field approach. The overviews of computational techniques, its advantages and disadvantages can be found in refs 14 and 28. Here, we mention the finite-field approach[33] that has become widespread in fullerene polarizability studies. According to this approach, the elements of the polarizability tensor are calculated as the second order derivatives of the total energy U with respect to the homogenous external electric field $\boldsymbol{E}$ (*i.e.* the field gradient and higher derivatives are zero):

$$\alpha_{ij} = -\frac{\partial^2 U}{\partial E_i \partial E_j} \qquad (11)$$

This approach is well combined with DFT techniques and allows calculating static polarizabilities, which, in general, are enough for chemical and materials science applications.

3 Polarizability of fullerenes and related structures

3.1 Fullerene polarizability

Fullerenes are highly polarizable molecules. This was confirmed by numerous experimental and theoretical methods.[20–22,34–57] Currently, the experimental data are available only for the C_{60} and C_{70} fullerenes whereas polarizabilities of the representatives of the fullerenes family from C_{20} to C_{2160} have been calculated in terms of the diverse approaches.[34–57] Among them, DFT-calculations provide the most trustworthy values. We have superposed the most credible data on the selected fullerenes in Table 1. The measured mean polarizability values of C_{60} and C_{70} are ~80 and ~105 Å^3, respectively. Note that some experimental works give unreliably high values for C_{60}. For example, such a value (~1000 Å^3) has been obtained in refs 58 and 59 that may be caused by the influence of impurities on the measurements, the unaccounted aggregation of the C_{60} molecules or possible formation of charge-transfer complexes, which significantly increase polarizability.[60]

Comparison of the most widespread density functionals PBE and B3LYP, applied to the fullerenes, demonstrates the higher efficiency of the first one for calculating α because the B3LYP-based methods underestimate the C_{60} polarizability (see, *e.g.*, refs 53 and 56) (Table 1). This is also true for M06-2X density functional and the long-range corrected schemes (*e.g.*, LC-wPBE).[61] The use of the mentioned functionals with the extended basis sets allows avoiding the underestimation. For example, in the case of M06-2X density functional, the extension of the basis set from 6-31G(d) to 6-31+G(d,p) leads to the increase in the calculated value of the C_{60} mean polarizability from 67.3[61] to 78.4[55] Å^3, respectively. In our studies, we prefer the PBE/3ζ method that quantitatively reproduces experimental values of the polarizability of fullerenes, as well as the spectral data (IR and NMR) of C_{60}/C_{70} and their derivatives.[45,62–65] In addition, semiempirical methods, specially parameterized to reproduce molecular properties of polycyclic hydrocarbons and fullerenes, are developed.[47]

Table 1 Static polarizabilities of fullerenes, a comparison between theoretical methods and experimental data (Å^3) [a]

Molecule	Theoretical estimations	Experimental data
C_{60} (I_h)	78.8 (CPHF/(7s4p)[3s2p]),[35] 75.1 (HF/6-31 ++G),[36] 83.0 (topological model),[39] 77.5 (point dipole interaction model),[40] 75.7 (bond order model),[41] 82.7 (PBE/3ζ),[45] 82.1 (PBE/NRLMOL),[46] 82.9 (QSRP model),[49] 81.6 (PBE0/SVPD),[51] 78.4 (VWN/DZVP/GEN-A2),[52] 80.3 (B3LYP/Λ1),[53] 78.4 (M06-2X/6-31+G(d,p),[55] 71.7 (B3LYP/6-31G(d))[56]	76.5±8.0 (molecular beam deflection),[22,38] 79.0±6.0 (time-of-flight technique),[37] 88.9±6.0 (interferometry)[42]
C_{70} (D_{5h})	93.2 (CPHF/(7s4p)[3s2p]),[35] 89.8 (HF/ 6-31 ++G),[36] 88.3 (bond order model),[41] 103.0 (PBE/NRLMOL),[43] 102.7 (PBE/3ζ),[44] 93.6 (QSRP model),[49] 97.8 (VWN/DZVP/GEN-A2),[52] 100.7 (B3LYP/Λ1)[53]	101.9±13.9 (molecular beam deflection),[38] 108.5±8.2 (interferometry)[42]
C_{76} (D_2)	112.3 (PBE/3ζ)[50]	–
C_{78} (D_3)	115.3 (PBE/3ζ)[50]	–
C_{80} (I_h)	129.4 (PBE/3ζ)[57]	–
C_{84} (D_{2d})	124.1 (PBE/3ζ),[50] 113.3 (CPHF/(7s4p)[3s2p])[35]	–
C_{90} (C_{2v})	135.8 (PBE/3ζ)[57]	–
C_{100} (D_5)	169.0 (PBE/3ζ)[57]	–
C_{120} (T_d)	189. 8 (PBE/3ζ)[57]	–
C_{240} (I_h)	441.0 (PBE/NRLMOL)[48]	–
C_{540} (I_h)	1192.6 (PBE/NRLMOL),[46] 1243.8 (PBE0/SVPD),[51] 1254.0 (VWN/DZVP/GEN-A2),[52]	–

[a] Other summarizing tables can be found in refs 47, 49, and 54.

For example, PM6 calculations[47] have been used to obtain good correlations of dynamic polarizabilities of C_{60} and C_{70} with ω (all values in a.u.):

$$\alpha_{C_{60}} = 530\left(1 + 13\omega^2 + 1020\,\omega^4\right) \qquad (12)$$

$$\alpha_{C_{70}} = 645\left(1 + 19\omega^2 + 5832\omega^4\right) \quad (13)$$

High mean polarizabilities of fullerenes are obviously caused by their rich π-electronic systems. Polarizability nonlinearly increases with the number of carbon atoms in the fullerene molecule and, consequently, with the number of readily polarizable π-bonds. This can be clearly demonstrated by polarizability per atom values α/N_C that grow up from 1.368 and 1.471 Å^3 for C_{60} and C_{70} to 2.209 Å^3 for C_{540} (mean polarizabilities calculated with PBE/NRLMOL from refs 43 and 46). It is noteworthy that the analogous nonlinear enhancement of α is typical for one-dimensional and two-dimensional π-conjugated systems such as polyenes,[66] polyynes,[67] oligo[*n*]acenes,[68] and some conjugated oligomers.[69] Thus, fullerenes behave similar to the conjugated hydrocarbons in the context of the mean polarizability. To avoid misunderstanding, we should also mention a theoretical work that declares quantum-size effects for polarizability of the fullerenes family.[27] This work deals with the relation of two semiempirical estimations of polarizability, which ratio grows up to the critical size of the fullerene molecule and then diminishes. It does not mean that polarizability analogously behaves as it permanently increases with the fullerene size.

In addition, the fullerenes family has clear dependence of mean polarizability per atom on the size. It makes fullerenes outstanding among the other nanostructures, which usually do not demonstrate such trends (see, *e.g.*, DFT study on the gallium arsenide clusters[70]).

As predicted by the point dipole interaction model,[71] the dependence of carbon nanotube polarizability on its size has the saturation length. When the saturation value is achieved, no significant changes of mean polarizability and the longitudinal polarizability of the nanotube are observed. This differs from the case of fullerenes and polycyclic aromatic hydrocarbons though carbon nanotubes have almost the same structure.[66–69] To be strictly stated, this difference between fullerenes and nanotubes should be studied by higher level theoretical (*e.g.*, DFT) or experimental methods.

3.2 Fullerene polarizability and physicochemical processes

Estimation of intermolecular interactions is the nearest application of the measured and calculated polarizabilities of fullerenes. For example, the dispersion interaction is a universal interaction that arise between the molecules. Its energy can be calculated as

$$U_{disp} = -\frac{C_6}{R^6}, \quad (14)$$

where C_6 is a dispersion interaction constant.[14,29] It is calculable in terms of different approaches. Most of them state the dependence of C_6 on the polarizabilities of the participants of interaction molecules ($C_6 \sim \alpha_1, \alpha_2$). Thus, the accurate calculation of C_{disp} has been performed by Kumar and Thakkar[72] via Casimir–Polder equation (Table 2), in which the imaginary parts of polarizability ($i^2 = -1$) are used:

$$C_6 = \frac{3}{\pi}\int_0^\infty \alpha_1(iy)\alpha_2(iy)dy \quad (15)$$

Table 2 Dispersion interaction coefficients C_6 for C_{60}…X interactions, a.u. Reprinted with permission from ref 72 © 2011 Elsevier

X	C_6	X	C_6
H	801.7	Propanol-1	9841
He	364.7	H_2CO	4052
Ne	737.3	CH_3CHO	6321
Ar	2511	$(CH_3)_2CO$	8885
Kr	3592	SF_6	7343
Xe	5362	SiH_4	5850
Li	8066	SiF_4	5561
H_2	1098	NH_2CH_3	5499
N_2	2674	$NH(CH_3)_2$	8031
O_2	2434	$N(CH_3)_3$	1.029×10^4
Cl_2	6230	C_2H_4	5479
HF	1341	Propene	8135
HCl	3604	Butene-1	1.063×10^4
HBr	4654	CCl_4	1.421×10^4
CO	2834	CH_4	3593
CO_2	3938	C_2H_6	6165
NO	2605	C_3H_8	8745
N_2O	4269	*n*-C_4H_{10}	1.124×10^4
C_2H_2	4519	*n*-C_5H_{12}	1.377×10^4
O_3	4111[a]	*n*-C_6H_{14}	1.624×10^4
SO_2	5399	*n*-C_7H_{16}	1.873×10^4
CS_2	9300	*n*-C_8H_{18}	2.122×10^4
SCO	6347	$O(CH_3)_2$	7284
H_2S	4652	$CH_3C_3H_7$	1.248×10^4
H_2O	2110	$O(C_2H_5)_2$	1.247×10^4
NH_3	2982	C_6H_6	1.313×10^4
CH_3OH	4690	C_{60}	1.003×10^5
C_2H_5OH	7290		

[a] The average of two estimations is given.

The obtained numerical data[72] make up valuable source for comparative estimation of van der Waals interactions of the buckminsterfullerene.

High α values of fullerenes have been used to qualitatively explain the distinctiveness of physicochemical processes in fullerene-containing systems such as the anomalously effective quenching of electronically-excited states of organic compounds by C_{60} and C_{70},[44] propensity of fullerenes for aggregation,[73] formation of the donor–acceptor complexes,[74] and behavior of the atoms, encapsulated by fullerene cages[75] (including their photoionization[76]). For example, Bulgakov and

Galimov have discovered that C_{70} is substantially more effective quencher from electronically excited states owing to energy transfer than C_{60}.[44] In these processes, C_{60} and C_{70} accept energies of the excited states of organic molecules according to inductive resonant mechanism:

$$C_{60} + D^* \rightarrow [C_{60}\ldots D]^* \rightarrow C_{60}^* + D \quad (16)$$

$$C_{70} + D^* \rightarrow [C_{70}\ldots D]^* \rightarrow C_{70}^* + D \quad (17)$$

According to the conventional notions,[77] each of the interactions above is considered as a resonant interaction of two oscillators (energy donor and energy acceptor). Donor and acceptor perturb the electronic structures of each other. Therefore, the different deactivating capabilities of C_{60} and C_{70} are explained with the unequal energies of the dipole–dipole interaction W:

$$W = \frac{1}{R^3}\left\{(\mu_D, \mu_A) - \frac{3}{R^3}(\mu_D R)(\mu_A R)\right\}, \quad (18)$$

where μ_D and μ_A are dipole moments of the donor D and acceptor A molecules and R is intermolecular distances. In comparative experiments,[44] the donors (*e.g.*, polycyclic hydrocarbons) were the same in the pairs $C_{60}\ldots D$ and $C_{70}\ldots D$; *i.e.* μ_D and R were constant in eqn (18). Thus, the difference in quenching is a consequence of the different dipole moments of C_{60} and C_{70}. These are both equal to zero in the ground state. However, in eqn (18), we should operate with the dipole moments of the excited states, which are hardly computable for such large molecules as fullerenes. We have proposed that the excited state dipoles are correlated with the dipoles, induced by external electric fields. The last ones, according to eqn (2), depend on polarizability. Numerous theoretical and experimental works demonstrate that C_{70} is more polarizable than C_{60}. Thus, the larger efficiency of the C_{70} fullerene as a quencher is attributed to the higher mean polarizability of its molecule.[44] We can expect that the larger fullerenes, having higher mean polarizabilities, may exhibit higher capabilities for quenching.

Polarizability is also useful for estimation of the conditions for ordering carbon nanostructures (higher fullerenes and nanotubes) in a polymer matrix under external electric fields.[78] The authors[78] have deduced formulae for estimation of time t_F, required for rotation of carbon nanostructure on the angle ϑ in the field E:

$$t_F = \frac{8\pi r^3}{\varepsilon_0 \alpha E^2} \ln|tg\,\vartheta| \quad (19)$$

and the condition for the electric field magnitude, required to perform ordering:

$$E \geq \frac{1}{\theta}\sqrt{\frac{4kT}{\varepsilon_0 \alpha}\ln|tg\,\vartheta|}, \quad (20)$$

where r is radius of the sphere with the volume, equal to the volume of the considered carbon nanostructure, and η is viscosity of the medium. Use of these conditions demonstrated that polarizabilities of C_{70} and C_{82} are insufficient to perform their ordering in low electric fields. In the case of nanotubes, which are more polarizable than fullerenes, the field 10^5 V cm^{-1} is able to rotate them on the angle ϑ = 60° in polymer medium.[78]

3.3 Fullerene polarizability *versus* fullerene reactivity

Analysis of reactivity of the fullerene molecules makes up another application of their polarizabilities. Two reasons underlie the usefulness of polarizability for this purpose.[79] First, the buckminsterfullerene readily forms various molecular complexes with[74] or without[80] charge transfer). In addition, quantum-chemical studies of potential energy surfaces of 1,3-dipolar cycloaddition to C_{60} show that it occurs through the pre-reactionary complexes (for example, in the case of ozone addition to C_{60}[45,81,82] and C_{70}[45]). Moreover, a key role of dispersion interaction for $C_{60}\ldots O_3$ stabilization has been demonstrated.[83] High polarizability of C_{60} also defines stability of analogous complexes with other species. Moreover, the enhanced stability of van der Waals complexes is able to prevent the further chemical interaction when both of the interacting molecules are highly polarizable (*e.g.*, C_{60}–iodine[84] and C_{60}–sulphur complexes[85]).

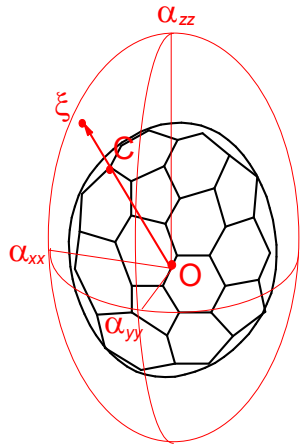

Fig. 1 Polarizability ellipsoid of the fullerene molecule. O is a center of mass, C is an atom on the fullerene surface, ξ is a point on the polarizability ellipsoid.[86]

Second, some classic concepts consider eigenvalues the polarizability tensor as semiaxes of polarizability ellipsoid, which covers the molecule and roughly represents its electronic cloud.[29] In the case of fullerenes, such an ellipsoid replicates the shape of a fullerene molecule.[86] To use polarizability for theoretical study of chemical properties, we have considered the fullerene molecule and its polarizability ellipsoid together in a polar coordinate system (with the origin at the center of mass of the fullerene) (Figure 1). This allowed assigning a point on

the ellipsoid and ascribing the index ξ to each reaction site of the molecule:[50,86]

$$\xi = \left(\frac{\sin^2\psi\cos^2\varphi}{\alpha_{xx}^2} + \frac{\sin^2\psi\sin^2\varphi}{\alpha_{yy}^2} + \frac{\cos^2\psi}{\alpha_{zz}^2} \right)^{-0.5} \quad (21)$$

where ξ is the polarizability in the direction of the reaction site with polar coordinates ψ and φ. In the case of the highly symmetric C_{60} molecule, all the indices are the same, being equal to its mean polarizability.

This approach have become useful for understanding the modes of ozone and diazomethane addition to higher fullerenes C_{70} (D_{5h}), C_{76} (D_2), and C_{78} (C_{2v}),[50] which have unequivalent double bonds in their structures in contrast to C_{60}. As is known, dipole molecules O_3 and CH_2N_2 react with 6.6 bonds of higher fullerenes that results in the formation of fullereno-1,2,3-trioxalanes and fulleropyrazolines (Figure 2).[87–90] The ξ indices are characterized atoms in the fullerene molecules. Additions of O_3 and CH_2N_2 to alkenes concertedly occur at two reaction sites,[91] so the polarizability indices of the bond Ξ have been calculated as the arithmetic mean:

$$\Xi = 0.5\ (\xi_1 + \xi_2) \quad (22)$$

For all the fullerenes, the calculated Ξ indices are within the range $\alpha_{ii}^{(min)} \le \Xi \le \alpha_{ii}^{(max)}$, characteristic for each fullerene ($\alpha_{ii}^{(min)}$ and $\alpha_{ii}^{(max)}$ are the smallest and highest eigenvalues of the polarizability tensor). As it turned out, the DFT-calculated heats of reactions of each fullerene increase with the Ξ value. In the case of the C_{70} fullerene, the *ab* and *cc* bonds, located near the poles of the molecule, have the largest Ξ indices (107.6 and 103.0 Å^3, respectively) (Figure 3). The heats of the reactions of 1,3-dipolar addition to these bonds are higher than those of the addition to the *de* and *ee* bonds. The *ab* and *cc* modes of addition are characterized with the lowest activation barriers and the corresponding trioxolanes *ab*-$C_{70}O_3$ and *cc*-$C_{70}O_3$ have been experimentally detected among the products of the C_{70} ozonolysis.[90] It is important that Ξ indices of the *ab* and *cc* bond exceed mean polarizability of C_{70} whereas in the case of the inert *de* and *ee* bonds, it is lower than that. Ξ-criterion of reactivity Ξ > α works well in the case of the other fullerenes.

The advantage of this approach is that both theoretical and experimental data on fullerene structure and polarizability are suitable for calculation of polarizability indices.[79] Later, we have extrapolated this approach to oxidation of the C_{60} derivatives $C_{60}O$ and $C_{60}F_{18}$, which also have different bonds in the structure.[92] Unfortunately, analysis of polarizability tensor is not the optimal way for theoretical studies of chemical properties of fullerenes and their derivatives. The calculated ξ (Ξ) indices allow considering the reaction sites of each fullerene separately,[93] *i.e.* these do not provide opportunities to cover the reactivity of the whole fullerenes family by the only correlation (as it is possible in the case of curvature indices and pyramidality angles[63,79,94–96]). Another disadvantage of this approach is ignoring the type of the adding particle. Thus, the addition of labile intermediates (radicals[97] and carbenes[98]) to the C_{70} fullerene takes place through atoms or bonds, which are "disfavored" in terms of polarizability (and curvature).

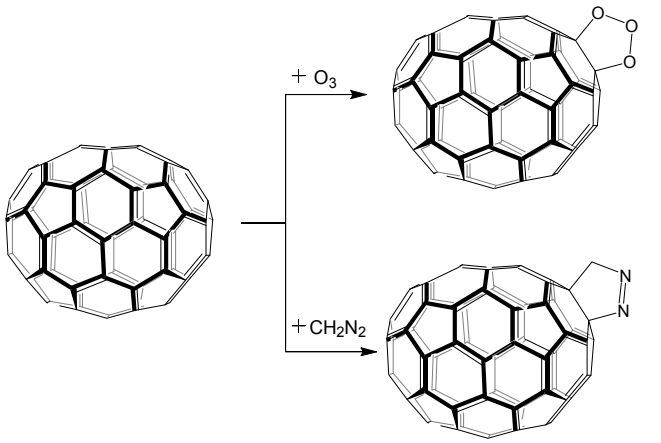

Fig. 2 Addition of ozone and diazomethane to the most reactive *ab* bonds of C_{70}.

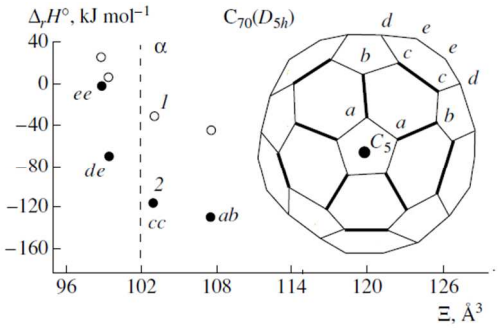

Fig. 3 Correlations of the heats of addition of diazomethane (*1*) and ozone (*2*) to C_{70} and the polarizability indices of the 6.6 bonds. Adapted with permission from ref 50 © 2009 Springer

3.4 Polarizability of the related carbon nanostructures, reactions therein and nanocapillarity

Unusual polarizability of fullerenes has triggered analogous studies of the related carbon nanostructures, which are inorganic fullerenes,[99] fullerenes with defects,[100] heterofullerenes,[100,101] carbon[71,102–104] and inorganic[105–107] nanotubes. Thus, the brightest examples of the use of their polarizabilities for understanding of physicochemical phenomena should be mentioned in a context of fullerene materials science.

As is known, nanotubes can play role of the thinnest capillaries, which can be filled with guest atoms, ions, or molecules. For example, open carbon nanotubes have been filled with molten $AgNO_3$[108,109] using capillarity forces. The process of filling has been analyzed in terms of the approach that links wetting with polarizability.[110] If van der Waals forces dominate the interface interaction (chemical interaction and/or charge transfer are absent), the contact angle of wetting θ_c depends on the polarizabilities of the wetting liquid α_L and wetted solid α_S:

$$\cos\theta_c = \frac{2\alpha_S}{\alpha_L} - 1 \quad , \qquad (23)$$

Consequently, the condition for wetting $\theta_c < 90°$ is achieved when $\alpha_L > 2\alpha_S$.[108,110] The authors[108] have also provided the expression for estimation of the polarizability of inner cavities α_{cav} of the curved graphitic surface (it is suitable for carbon nanotubes and may be extrapolated to fullerenes):

$$\alpha_{cav} = \alpha_{gr}(1 - 0.0275\theta_P) \quad , \qquad (24)$$

where α_{cav} is the planar graphitic polarizability and θ_P is pyramidality angle, which defines the diameter of the nanotube. Combination of eqns (23) and (24) allows predict the appropriate diameter for nanotube, which may be facilely filled with desirable compounds by capillarity forces.[108,109] Note that Pederson *et al.*[111,112] have computationally studied polarizabilities of carbon nanotubes and predicted their use as molecular straws before the discussed experiments.

Inner cavities of carbon nanotubes provide additional opportunities of carrying out chemical reactions in the nano-sized reactors.[113–118] When such reactions in the confined spaces are quantum-chemically studied, one should take into account the influence of the carbon framework on the reaction paths. The use of polarizable-continuum models[119] is the easiest way to do that. Such models require knowledge of dielectric permittivity of the medium ε, that is, in our case, a nanotube. To perform quantum chemical study on the Menshutkin reaction inside (8,0) and (9,0) carbon nanotubes within this approach, the authors[113] have estimated ε by Clausius–Mossotti formula:

$$\varepsilon = 1 + \rho\alpha\left(1 - \frac{\rho\alpha}{3}\right)^{-1} + \frac{\rho^2\alpha^2}{3} \quad , \qquad (25)$$

where ρ is a density, which is also a computable property. In addition, the works denote the influence of the polarizability of the nanotube reactor on the chemical behavior of the encapsulated reactants.[113,114,118]

Currently, processes of "nano-wetting" and chemical reactions inside fullerenes are mainly hypothetical. However, approaches to make them possible, such as molecular surgery,[120] are rapidly developed. For example, molecular surgery consists of chemical opening the cages, putting a desirable molecule inside, and restoring the initial structure of the cage. Endofullerenes $H_2@C_{60}$, $H_2O@C_{60}$, and analogous compounds has been successfully produced by this methodology.[120–122] In this context, carrying out chemical reactions inside higher fullerenes and capillarity-assisted filling them are possible in the nearest future.

4 Polarizability of exohedral derivatives with simple (non-fullerene) addends

4.1 Polarizability of fullerene monoadducts

Polarizability of fullerene derivatives has been studied mainly by theoretical techniques[8,53,56,92,123–137] because of many reasons such as their possible dissociation under experiments, low solubility, and low availability. The only experimental work in this field deals with the optical polarizabilities of polyfluoro[60]fullerenes measured by Tau–Talbot–Kapitza–Dirac interferometry.[138] As is known from the theoretical studies, mean polarizabilities of exohedral fullerene derivatives are higher than the polarizability of the original fullerene if its carbon framework does not degrade upon chemical functionalization.[8,53,56,92,123–137] This is true for both mono- and polyadducts, produced by [1+1]-addition or [2+*n*]-cycloaddition to C_{60},[8,53,56,92,123,125–128,131,132,134,135] C_{70},[53,131,133,136,137] C_{50},[124] or C_{56}[130] fullerenes. Mean polarizabilities of the typical C_{60} monoadducts are listed in Table 3.

It is well-known that [2+1]-addition to C_{60} and C_{70} leads to two types of adducts, *viz*. 6.6-closed (addition to 6.6 bond) and 5.6-open (addition to 5.6 bond with its simultaneous cleavage) (Figure 4).[89] 5.6-Open derivatives are usually formed in a mixture with their 6.6-closed isomers in the same reactions and then convert to them spontaneously or under thermal treating[89,140] (here, we do not consider 6.6-open fullerene adducts; in general, these unexpected products of addition are unstable[140]). In the case of C_{60} adducts, the mean polarizability of a 5.6-open isomer exceeds the polarizability of their 6.6-closed counterpart on ~0.5 Å^3 (Table 4). It is explained by the contribution of π-electronic system to polarizability of the studied molecules: because all 6.6 double bonds remain unbroken in 5.6-open derivatives (*i.e.* the initial π-electronic system does not change significantly), they are characterized with higher α values than respective 6.6-closed isomers.

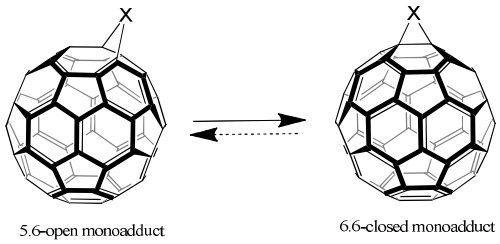

Fig. 4 5.6-Open–6.6-closed isomerization of fullerene adducts. The reverse reaction is hypothetical and shown by dashed arrow.

Table 3 Mean polarizabilities of C_{60} monoadducts, calculated by DFT methods (Å^3)

Molecule	α (Method and reference)
Cyclopropafullerenes	
R = R′ = H	85.0 (PBE/3ζ)[131]
R = R′ = COOH	91.7 (PBE/3ζ)[8]
R = C_6H_5, R′ = $(CH_2)_3COOCH_3$ (PCBM)	108.4 (PBE/3ζ),[8] 85.6 (B3LYP/3-21G*)[126]
Pyrrolidinofullerenes	
R = R′ = H	89.0 (PBE/3ζ)[135]
R = CH_3, R′ = H	77.3 (B3LYP/6-31G*)[125]
R = CH_3, R′ = –*p*-$C_6H_4NH_2$	96.5[a] (B3LYP/6-31G(d))[56]
R = CH_3, R′ = –*p*-$C_6H_4NO_2$	100.1[a] (B3LYP/6-31G(d))[56]
R = CH_3, R′ = –*p*-C_6H_4NO	100.8[a] (B3LYP/6-31G(d))[56]
	99.1 (PBE/3ζ)[135]
(iso-PCBM)	109.0[b] (PBE/3ζ)

[a] α(C_{60}) = 71.7 Å^3, calculated with the same method.

[b] Calculated specially for the review with the finite-field methodology, applied to PCBM previously.[8] The chosen for this purpose, PBE/3ζ method gives heat effect of the transformation PCBM → iso-PCBM equal to –37.4 kJ mol^{-1}. This is in perfect agreement with the previous estimations of the relative stabilities (iso-PCBM is 41.7–44.5 kJ mol^{-1} more stable than PCBM according to the quantum-chemical calculations with DFT and Møller–Plesset perturbation methodologies).[139]

This regularity is also typical for 6.6-closed and 5.6-open monoadducts of C_{70} (Figure 5). This has been numerically demonstrated on the example of its epoxides (6.6-closed) and oxafullereoids (5.6-open), which can be produced in a mixture at the C_{70} liquid-phase ozonolysis.[90] According to PBE/3ζ calculations,[131] all the $C_{70}O$ oxafulleroids have the larger mean polarizabilities (Figure 5).

Table 4 Mean polarizabilities and their splits for $C_{60}X_n$ (n = 1 and 6) and $C_{70}X$ isomers with 5.6-open and 6.6 closed moieties (in Å^3; PBE/3ζ calculations).

Fullerene adduct	Mean polarizability		Δα split
	$\alpha_{5.6\text{-open}}$	$\alpha_{6.6\text{-closed}}$	
$C_{60}O$ [a]	83.2	83.9	0.7
$C_{60}NH$ [a]	84.2	84.8	0.5
$C_{60}CH_2$ [a]	85.0	85.5	0.6
$C_{60}O_6$ [b]	89.3	85.2	4.1
$C_{60}(NH)_6$ [b]	95.6	90.7	4.9
$C_{60}(CH_2)_6$ [b]	99.3	94.8	4.5

[a] Taken from ref 131.

[b] Hexakisadducts with uniform distribution of addends on the fullerene cage. Taken from ref 9.

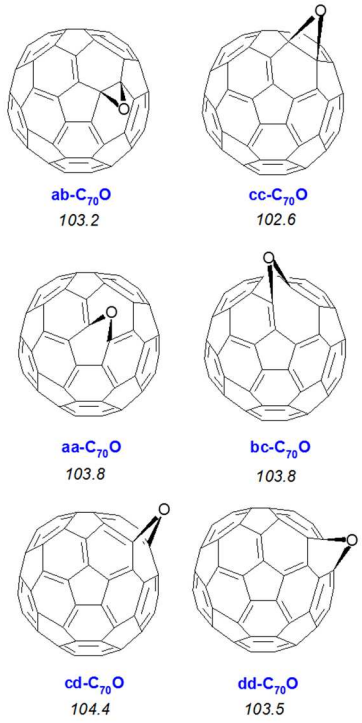

Fig. 5 Epoxides and oxidoannulenes, produced by the C_{70} ozonolysis. Mean polarizabilities are in Å^3 (PBE/3ζ calculation[131]).

4.2 Polarizability of fullerene bis- and multiadducts. Influence of isomerism

6.6-Closed–5.6-open isomerism in the case of monoadducts has been considered in the section above. When fullerene adducts with larger number of the attached addends are considered, positional isomerism emerges (Figure 6). Reactions of addition to fullerenes usually result in the mixture of the adducts $C_{60}X_n$ with variable n.[89,140] For example, the numbers of bisepoxifullerenes $C_{60}O_2$ and trisepoxifullerenes $C_{60}O_3$ equal to 8 and 47, respectively.[141]

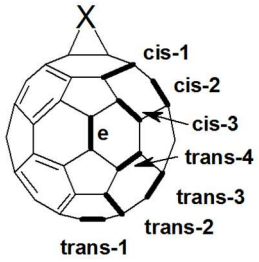

Fig. 6 Positional isomerism of C_{60} bisadducts. Possible positions of the second addend in $C_{60}X_2$ are denoted.

In our works, we have theoretically investigated mean polarizabilities of the positional isomers of $C_{60}X_2$ with the simplest addends by PBE/3ζ method.[8,53,132] As it turned out, mean polarizabilities of isomeric bisepoxy-, bisaziridino- and biscyclopropa[60]fullerenes (X = O, NH, and CH_2, respectively) are approximately equal (~84, ~86 and ~87 Å^3, respectively). This rule holds true for [2+3]- and [2+4]-adducts of C_{60}[135] as well as for multiadducts with greater number of addends.[132] According to DFT-calculations,[132] the mean polarizabilities of $C_{60}X_6$ (X = CH_2 and NH) isomers with compact, focal or uniform distributions of X moieties on a fullerene framework do not differ significantly (Figure 7).

In the case of the substituted cyclopropa[60]fullerenes, mean polarizability remains regardless of positional relationship of the addends attached. We have demonstrated it on the example of two "carboxyfullerenes" – *t*,*t*,*t*- и *e*,*e*,*e*-tris(dicarboxymethano)fullerenes.[8] These species are produced via reaction of fullerene with malonic ester derivatives[142] and attract a great interest due to their physiological activity, *e.g.*, inhibition activity towards some enzymes[143]). In spite of the different patterns of additions in these compounds, their mean polarizabilities are almost equal (Figure 8). Their high polarizabilities allows explaining strong propensity for aggregation in solutions, previously studied.[144]

The analogous situation is typical for isomeric halofullerenes $C_{60}Hal_n$,[53] formally considered as [1+1] adducts (Table 5). Most of them are produced as mixtures of several isomers. Moreover, isomerization processes are able to take place in halogen-containing fullerene derivatives. For example, a slow room-temperature interconversion of C_1 and C_3 isomers of $C_{60}F_{36}$ occurs in the presence of ambient atmosphere.[145] Carbon skeletons of the fluorinated matters changes insignificantly upon the isomerization:[146]

$$C_1\text{-}C_{60}F_{36} \leftrightarrow C_3\text{-}C_{60}F_{36} \qquad (26)$$

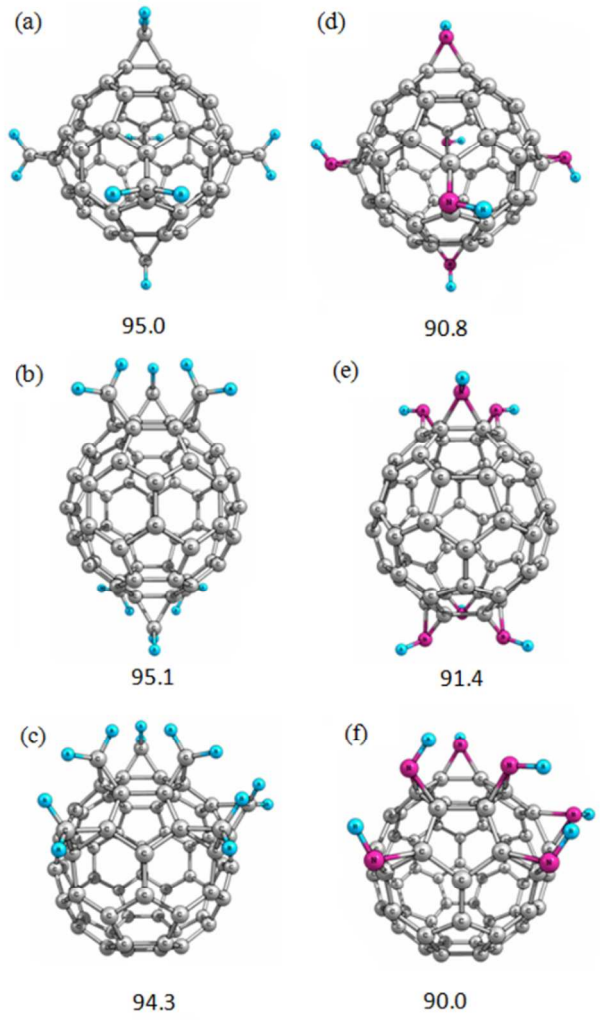

Fig. 7 Hexakisadducts $C_{60}(CH_2)_6$ (a–c) and $C_{60}(NH)_6$ (d–f) with uniform (a, d), focal (b, e), and compact (c, f) distributions of X groups on the fullerene cage and their mean polarizabilities, calculated by the PBE/3ζ method (Å^3). Reprinted with permission from ref 132 © 2012 Elsevier

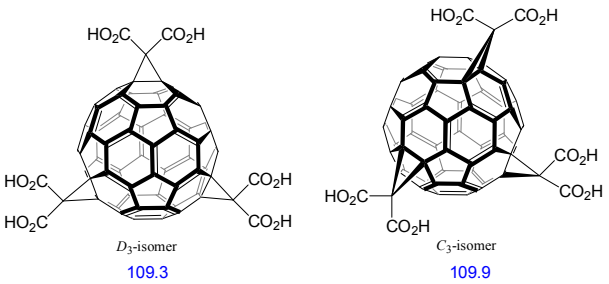

Fig. 8 Regioisomeric carboxyfullerenes. Mean polarizabilities, calculated by the PBE/3ζ method,[8] are shown in Å^3.

Isomeric $C_{60}Hal_n$, differing by the relative Hal positions, are characterized by approximately the same values of mean polarizability, *e.g.*, for all $C_{60}F_{36}$ isomers α equals to ~89 Å^3 (Table 5). However, the third isomer *T*-$C_{60}F_{36}$ has the carbon skeleton, far from the mentioned isomers, whereas it has the same α. The difference in mean polarizability achieves the

highest value for two $C_{60}Cl_{30}$ isomers (~10 Å^3) with dissimilar geometries of carbon frameworks. In addition, the structure of isomer with higher polarizability D_{3d}-$C_{60}Cl_{30}$ is characterized by the trannulene equatorial belt, which made up by facilely-polarizable conjugated double bonds (Figure 9).

Considering the above, we can conclude that, usually, positional isomerism negligibly effects on mean polarizability of fullerene adducts. However, in rare cases, it can lead to a considerable difference in mean polarizabilities of the positional isomers.

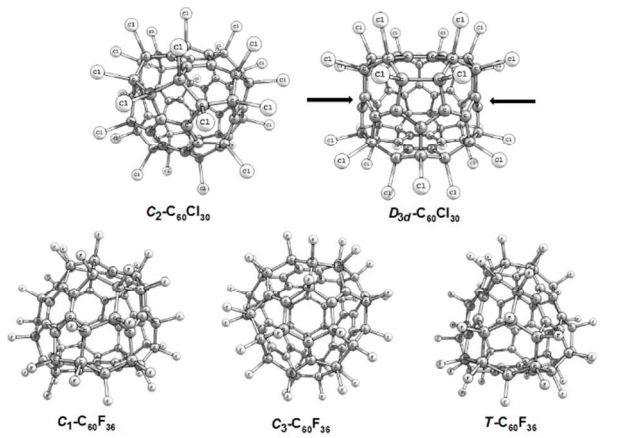

Fig. 9 Isomeric $C_{60}Cl_{30}$ and $C_{60}F_{36}$ halofullerenes. Trannulene equatorial belt in D_{3d}-$C_{60}Cl_{30}$ (a system of π-conjugated bonds) is marked by arrows.

Table 5 Mean polarizabilities of halofullerenes, calculated by the PBE/3ζ method[53] (in Å^3)

Molecule	α	Molecule	α
1,2-$C_{60}F_2$	84.0	1,2-$C_{60}Cl_2$	89.6
C_s-$C_{60}F_{16}$	87.8	C_s-$C_{60}Cl_6$	100.7
C_{3v}-$C_{60}F_{18}$	87.4	T_h-$C_{60}Cl_{24}$	140.2
D_{5d}-$C_{60}F_{20}$	88.4	C_1-$C_{60}Cl_{28}$	149.4
T_h-$C_{60}F_{24}$	84.7	D_{3d}-$C_{60}Cl_{30}$	161.0
C_1-$C_{60}F_{36}$	88.8	C_2-$C_{60}Cl_{30}$	150.4
C_3-$C_{60}F_{36}$	88.8	1,2-$C_{60}Br_2$	92.9
T-$C_{60}F_{36}$	89.0	C_{2v}-$C_{60}Br_6$	109.9
D_3-$C_{60}F_{48}$	90.5	C_s-$C_{60}Br_8$	119.6
S_6-$C_{60}F_{48}$	90.4	T_h-$C_{60}Br_{24}$	172.6

4.3 General formula for calculation of mean polarizability of fullerene exohedral derivatives

Polarizability of diverse multiadducts have been theoretically studied but the question of how polarizability of $C_{60}X_n$ depends on the number of addends n was unanswered for a long time. First, Hu and Ruckenstein estimated mean polarizabilities of the C_{60} fullerene and its hydrides $C_{60}H_2$ and $C_{60}H_{60}$ as 73.8, 74.7, and 77.9 Å^3, respectively (B3LYP/6-31G(d) calculations).[123] However, their study[123] was focused on endohedral structures, so they did not pay attention to the striking difference: formation of $C_{60}H_2$ from C_{60} increases mean polarizability of 0.9 Å^3 whereas the addition of the next 58 hydrogen atoms leads to the unexpectedly small increase (3.2 Å^3). Later, Rivelino *et al.* in the theoretical study of structures, stabilities, and light scattering of fullerenols $C_{60}(OH)_n$ have pointed that the mean polarizability grows up from $C_{60}(OH)_2$ to $C_{60}(OH)_{18}$ but then diminishes for $C_{60}(OH)_{24}$.[127] This work has explained this falling down by the highly symmetric addition pattern in $C_{60}(OH)_{24}$ compared to its precursor with 18 hydroxyls. However, as we have shown in Section 4.2, positional isomerism generally does not affect polarizability. Finally, we have found the same situation in the case of epoxy[60]fullerenes $C_{60}O_n$[131] (in the set with n up to 30, $C_{60}O_{15}$ has the maximal α).

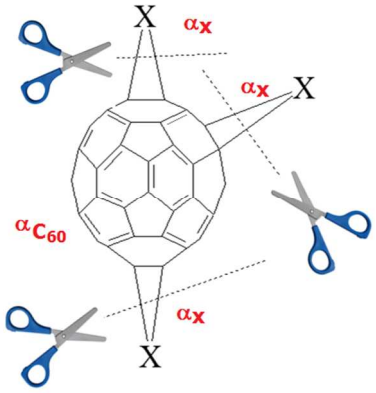

Fig. 10 Consideration of fullerene adducts in terms of additive scheme, described by eqns (26) and (27).[23]

To uncover this enigmatic behavior, we have scrutinized the $C_{60}X_n$ polarizabilities with DFT methods and careful additivity rules. We should mention that the development of the first one usually makes the additive approach unnecessary. Nevertheless, evaluation of additive polarizability has not lost its relevance in structural studies,[147] so we have compared our DFT-calculated polarizabilities within the additive scheme for cyclopropa-$C_{60}(CH_2)_n$ and aziridinofullerenes $C_{60}(NH)_n$ with n up to 30 (which is a number of double bonds in C_{60} molecule).[132] For this purpose, the only randomly chosen isomer has been selected for each n because, as mean polarizability is defined mainly by the number of addends. The following additive scheme has been applied. Each fullerene cycloadduct has been partitioned on (n + 1) subunits of two types: a fullerene cage and n addends attached (Figure 10). According to this scheme, additive polarizabilities of $C_{60}X_n$ equal to:

$$\alpha_{add}\left(C_{60}X_{n_{\max}}\right)=\alpha_{C_{60}}+n\alpha_X, \qquad (27)$$

where

$$\alpha_X=\alpha_{C_{60}X}-\alpha_{C_{60}} \qquad (28)$$

are increments (X are bivalent chemical moieties >CH_2 or >NH). Increments α_X describe the change in polarizability upon the addition of one X fragment, accompanied by disappearance of π-component of one 6.6 bond ($\alpha_X > 0$).

According to eqn (27), additive polarizabilities of $C_{60}(CH_2)_n$ and $C_{60}(NH)_n$ enlarge linearly when $n\rightarrow30$. As DFT

calculations show,[132] the differences between $\alpha(C_{60}X_n)$ and $\alpha_{add}(C_{60}X_n)$ become greater with n increase and we observe the depression of polarizability $\Delta\alpha$, *i.e.* the negative deviation of $\alpha(C_{60}X_n)$ from $\alpha_{add}(C_{60}X_n)$:

$$\Delta\alpha = \alpha_{add}\left(C_{60}X_n\right) - \alpha\left(C_{60}X_n\right) \quad (29)$$

For both classes of cycloadducts, $\Delta\alpha$ achieves maximal value at n = 30 (Figure 11). Based on mathematical induction, the computed data have been analyzed with a fitting function, which unites mean polarizability and number of addends in a fullerene derivative molecule:

$$\alpha\left(C_{60}X_n\right) = \alpha_{C_{60}} + n\alpha_X + \frac{\Delta\alpha\left(C_{60}X_{n_{\max}}\right)n^2}{n_{\max}^2}, \quad (30)$$

where two first terms of the equation make up the additive polarizability and $\Delta\alpha\left(C_{60}X_{n_{\max}}\right)$ is a depression of polarizability of the totally-functionalized fullerene derivative.[132] In this formula, the depression of polarizability for fullerene adduct with n addends is:

$$\Delta\alpha\left(C_{60}X_{n_{\max}}\right) = \frac{n^2}{n_{\max}^2}\Delta\alpha\left(C_{60}X_{n_{\max}}\right). \quad (31)$$

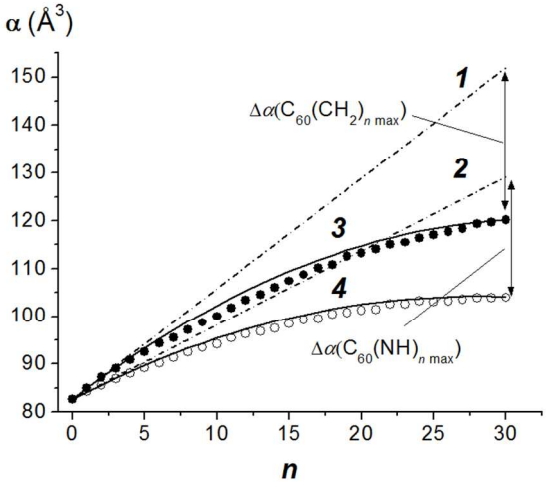

Fig. 11 Dependences of α on n values, obtained by PBE/3ζ method in terms of additive scheme without (1 – $C_{60}(CH_2)_n$, 2 – $C_{60}(NH)_n$) (eqn (27)) and with the correction on the depression of polarizability (3 – $C_{60}(CH_2)_n$, 4 – $C_{60}(NH)_n$) according to eqns (30) and (37). Black and white circles correspond to pure quantum-chemically calculated α values of $C_{60}(CH_2)_n$ and $C_{60}(NH)_n$, respectively. Reprinted with permission from ref 132 © 2012 Elsevier

We consider that this correction to the additive scheme has physical meaning. Previously,[8] we have interpreted it as follows. Rewriting eqn (31) as

$$\Delta\alpha\left(C_{60}X_{n_{\max}}\right) = \frac{\Delta\alpha\left(C_{60}X_{n_{\max}}\right)}{n_{\max}} \times \frac{n}{n_{\max}} \times n \quad (32)$$

allows demonstrating that depression of polarizability is proportional to specific depression (depression of the totally-functionalized fullerene derivative per one addend, the first term), degree of functionalization ($n/n_{\max}$, the second term), and the number of addends attached (the third term).

For this review, we have reanalyzed the computational data, obtained previously,[132] using combinatorial approach. The number of all possible interactions X…X in the $C_{60}X_n$ molecule equals to the number of double combinations:

$$C_n^2 = \frac{n!}{(n-2)!2!} = \frac{n(n-1)}{2}. \quad (33)$$

Then the specific depression of the totally-functionalized fullerene derivative equals to

$$\Delta\alpha\left(C_{60}X_{n_{\max}}\right)_{spec} = \frac{2}{n_{\max}(n_{\max}-1)}\Delta\alpha\left(C_{60}X_{n_{\max}}\right). \quad (34)$$

The depression of polarizability for the arbitrary $C_{60}X_n$ is calculated as

$$\Delta\alpha\left(C_{60}X_n\right) = C_n^2\Delta\alpha\left(C_{60}X_{n_{\max}}\right)_{spec}. \quad (35)$$

Substitution of eqns (33) and (34) in eqn (35) provides the final variant:

$$\Delta\alpha\left(C_{60}X_n\right) = \frac{n(n-1)}{n_{\max}(n_{\max}-1)}\Delta\alpha\left(C_{60}X_{n_{\max}}\right). \quad (36)$$

The last expression is very close to the mathematically induced eqn (31). However, eqn (36) is more justified. Indeed, consideration that the depression of polarizability is caused by the X…X interactions, we should obtain $\Delta\alpha = 0$ when $n = 0$ or 1. This is true only when we use eqn (36). Thus, we can finally writing the general equation for mean polarizability of the fullerene derivatives:

$$\alpha\left(C_{60}X_n\right) = \alpha_{C_{60}} + n\alpha_X + \frac{n(n-1)}{n_{\max}(n_{\max}-1)}\Delta\alpha\left(C_{60}X_{n_{\max}}\right) \quad (37)$$

Fitting functions (37) (and (30)) render the quantum-chemically obtained values of [2+1]-cycloadducts polarizability with high accuracy (Figure 11). Derived strictly for $C_{60}(CH_2)_n$ and $C_{60}(NH)_n$ cycloadducts, these formulae reproduce well the DFT-calculated mean polarizabilities of other derivatives of C_{60}[8,53] and C_{70},[53,133] *i.e.* it works for the other fullerenes (Figures 12 and 13) (Table 6).

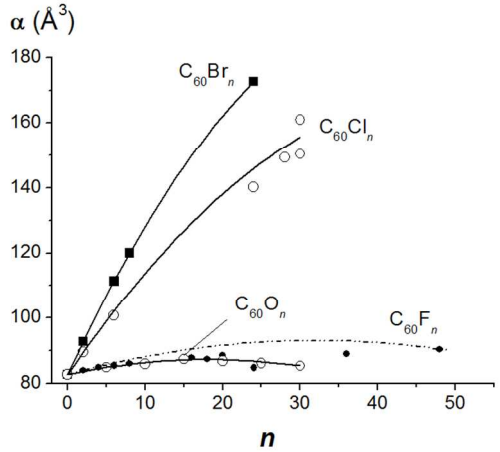

Fig. 12 Dependence of mean polarizability on the number of the attached atoms in fullerene derivatives (PBE/3ζ calculations). Symbols correspond to the pure quantum-chemically calculated mean polarizabilities; lines show dependences α *versus n*, obtained by the use of fitting functions (30) or (37). The calculated data have been taken from refs 53 and 131.

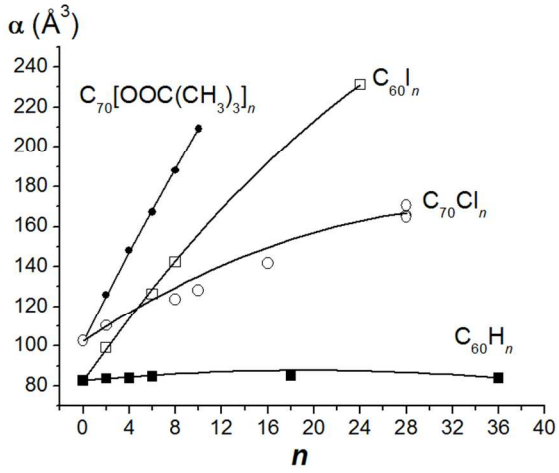

Fig. 12 Dependence of mean polarizability on the number of the attached atoms in fullerene derivatives (PBE/3ζ calculations). Symbols correspond to the pure quantum-chemically calculated mean polarizabilities; lines show dependences α *versus n*, obtained by the use of fitting functions (30) or (37). The calculated data have been taken from refs 8, 53, and 133.

The derived functions (30) and (37) have the respective maxima:

$$N_{\max}^{Eqn(29)} = -\frac{\alpha_X n_{\max}^2}{2\Delta\alpha\left(C_{60}X_{n_{\max}}\right)} \qquad (38)$$

and

$$N_{\max}^{Eqn(35)} = \frac{1}{2} - \frac{\alpha_X n_{\max}(n_{\max}-1)}{2\Delta\alpha\left(C_{60}X_{n_{\max}}\right)}. \qquad (39)$$

It means that the dependence of mean polarizability of fullerene adducts is generally nonmonotonic. This was previously found for $C_{60}(OH)_n$[127] and $C_{60}O_n$.[131]

This approach to interpretation of the computational data demonstrate efficiency in the cases of other derivatives of both C_{60} and C_{70} (Tables 6 and 7, Figure 12). Parameters of the corresponding fitting functions are collected in Table 6. It is noteworthy that formulae (30) and (37) work regardless the quantum-chemical method used.[53,132] In fact, it is applicable to $C_{60}(OH)_n$ polarizabilities, calculated by Rivelino *et al.*[127] with B3LYP/6-31G(d,p) (Figure 13). In this set, only $C_{60}(OH)_{18}$ violates the regularity. The reasons for this are addressed to the further studies.

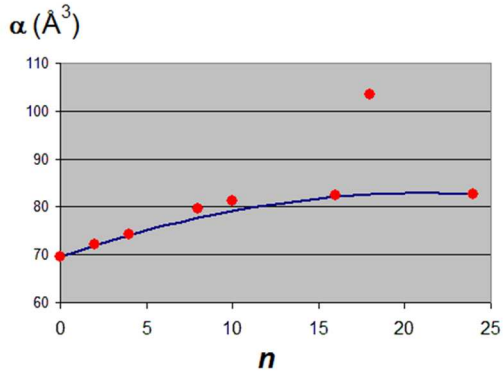

Fig. 14 Mean polarizability of the fullerenols family. Red points correspond to B3LYP/6-31G(d,p) values (taken from ref 127). Line shows calculation by eqn (37) with parameters, deduced from the mentioned quantum-chemical calculations.[127]

In our works, we pay particular attention to high-polarizability molecules, for example, iodo[60]fullerenes. As known, there are obstacles to synthesize fullerene derivatives with C–I bonds, possibly due to the constraints, arising between the voluminous iodine atoms. It makes the reaction of iodine with fullerene core thermodynamically unfavourable.[148] However, the iodination of C_{60} fullerene should lead to easily polarizable compounds, which have a strongly expressed response to external electric fields, because $C_{60}I_n$ have the highest mean polarizabilities among the other C_{60} derivatives. Attempts to the synthesis of the iodinated C_{60} are being performed.[149]

The disadvantage of our explaining the depression of polarizability and the derived general formulae should be noted. One of the parameters, defining Δα value according to eqns (30) and (37), is a maximal number of addends (n_{max}), which can be attached to fullerene skeleton. The n_{max} value is difficult to determine exactly (both experimentally and theoretically) whereas it is significant for the effective use of the mentioned formulae. Though the stability of some totally-functionalized fullerene derivatives has been clearly shown (*e.g.*, polyepoxide $C_{60}O_{30}$[150]), n_{max} = 30 is rather hypothetical value. Nevertheless, the use of both theoretically possible maximal value (n_{max} = 30) for [2+1]-cycloadducts and n_{max} values for [1+1]-adducts, experimentally known at the moment, demonstrates good agreement between our formula and DFT-calculations.

Table 6 Parameters of eqns (30) and (37) for calculation of mean polarizability of fullerene adducts

Fullerene adducts	α_X (Å^3)	$-\Delta\alpha(C_{60}X_{n_{max}})$ (Å^3)	n_{max}
$C_{60}(CH_2)_n$ [a]	2.31	31.8	30
$C_{60}(NH)_n$ [a]	1.55	25.2	30
$C_{60}O_n$ [a]	0.50	12.3	30
$C_{60}F_n$ [a]	0.65	23.5	48
$C_{60}Cl_n$ [a]	3.45	30.5	30
$C_{60}Br_n$ [a]	5.12	33.0	24
$C_{60}I_n$ [a]	8.17	47.8	24
$C_{60}H_n$ [a]	0.525	17.6	36
$C_{60}H_n$ [b]	0.90	49.9	60
$C_{60}(OH)_n$ [c]	1.26	17.2	24
$C_{70}Cl_n$ [a]	3.78	41.6	28
$C_{70}[OOC(CH_3)_3]_n$ [a]	11.51	8.7	10

[a] PBE/3ζ calculations. Taken from refs 8, 53, 131–133.

[b] B3LYP/6-31G(d) calculations. Taken from ref 123.

[c] B3LYP/6-31G(d,p) calculations. Taken from ref ref 127.

Table 7 Mean polarizability and depression of polarizability (in parentheses) of $C_{70}X_n$ (in Å^3; PBE/3ζ calculations). Reprinted with permission from ref 133 © 2012 Taylor and Francis

X	$C_{70}X_8$	$C_{70}X_{10}$
H	101.9 (–1.1)	102.1 (–1.0)
CH_3	116.9 (–8.6)	120 (–11.3)
C_6H_5	196 (–12.4)	217.8 (–17.09)
Cl	123.6 (–9.3)	128 (–12.5)
Br	137.5 (–10.8)	144.8 (–14.9)
$OOC(CH_3)_3$	188.1 (–6.6)	209.1 (–8.7)

There is the only experimental work where mean polarizabilities of two halofullerenes have been measured.[133] The experimental technique was based on Kapitza–Dirac–Talbot–Lau interferometry.[31,32] It allowed obtaining experimental data on $C_{60}F_{36}$ (60.3±7.7 Å^3) and $C_{60}F_{48}$ (60.1±7.5 Å^3), which correspond to the mixtures of isomers.[138] Nevertheless, as follows from the calculations (Table 5), the structure does not influence on the static mean polarizability of the studied polyfluorofullerenes (though it remains significant for evaluation of dipole moments). Despite the fact that DFT methods, used in refs 8 and 53, overestimate the respective measured values, both experimental and theoretical studies indicate the equality of $C_{60}F_{36}$ and $C_{60}F_{48}$ polarizabilities. A mismatch between the measured and calculated values may occur because the computation represents static polarizabilities while the experiment[8] yields the optical polarizability at 532 nm laser wavelength. The equality of experimental mean polarizabilities of polyfluorofullerenes with different numbers of addends[138] confirms our theoretical assumptions about depression polarizability.

4.4 Anisotropy of polarizability and its application to organic solar cells

As mentioned, mean polarizabilities of regioisomeric fullerene bis- and multiadducts are almost the same. Differences are observed for anisotropy of their polarizability (a^2). Dependences of a^2 on the internuclear distance between the central atoms of the attached moieties L for the simplest bisadducts are shown in Figure 6. Regioisomers are characterized by the different a^2 values. In the case of X = CH_2 and NH, the highest values of anisotropy are typical for *trans*-1-$C_{60}X_2$, and the smallest ones correspond to equatorial bisadducts *e*-$C_{60}X_2$ (bisepoxy[60]fullerenes fall out of this trend).[8]

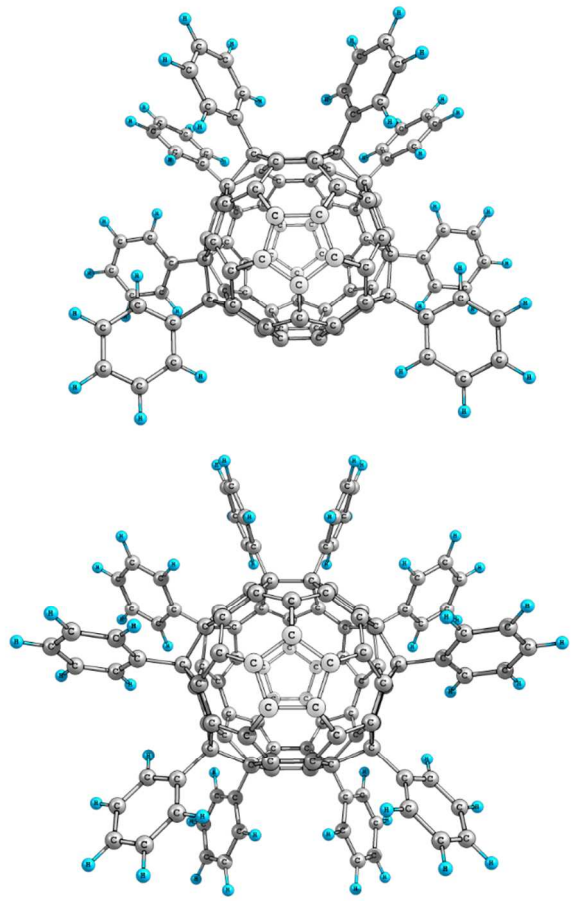

Fig. 15 Structures of $C_{70}Ph_8$ (top) and $C_{70}Ph_{10}$ (bottom). Polar pentagons, made up by atoms *a*, are whitened for clarity.

The C_{60} is initially isotropic and its decoration by functional groups leads to a violation of the isotropy that is reflected by the increase of a^2 values.[53] Upon the functionalization of C_{70}, which is initially anisotropic molecule (a^2 = 136.89 Å^6), the changes in anisotropy of polarizability depend on the nature of addends.[133] According to PBE/3ζ calculations, hydro[70]fullerenes $C_{70}H_8$ and $C_{70}H_{10}$ have the lower a^2 values (56.13 and 28.26 Å^6, respectively). Anisotropy enlarges in the case of the other C_{70} derivatives: the maximal values of anisotropy among the studied compounds characterize $C_{70}Ph_8$

and $C_{70}Ph_{10}$ (Figure 15). Anisotropies of polarizability and calculated increments α_X are cymbate values (Figure 16).[133]

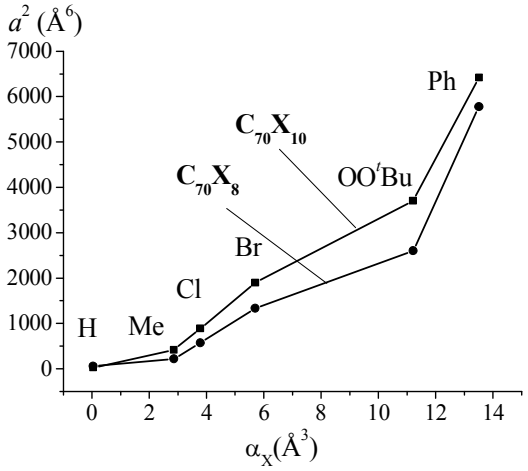

Fig. 16 Dependences of anisotropy of polarizability a^2 on α_X values for C_{70} derivatives (PBE/3ζ calculations). Reprinted with permission from ref 133 © 2012 Taylor and Francis

Thus, isomeric fullerene derivatives demonstrate approximately the same mean polarizabilities and differ by anisotropies. It may be useful for searching of new promising fullerene derivatives for diverse applications. For example, many novel compounds, including fullerene multiadducts, come into use as acceptor materials for organic solar cells.[151] Developing structure–property relationships may facilitate the screening of appropriate compounds for this purpose.

Previously, we have found a correlation between the anisotropies of polarizability of dihydronaphthyl-C_{60} bisadducts ($C_{60}dhn_2$) and the key output parameters of organic solar cells, based on them.[135] We have used the output parameters, measured in the same experimental protocols by Kitaura *et al.* for the isolated and purified derivatives of $C_{60}dhn_2$.[152] We pay particular attention to this pioneering study[152] because it utilizes the purified bisadducts in contract to the previous works, which deal with the mixtures of regioisomers. Note that the substituted $C_{60}dhn_2$ with alkylcarboxy chains ($-CO_2C_6H_{13}$) in naphthyl moieties were tested in experiments whereas the non-substituted $C_{60}dhn_2$ were quantum-chemically treated to facilitate the task. This simplification has been justified in the context of experimental study[153] of fullerene dendrimers, which have the same electrooptical properties regardless the number of generation. The devices with the derivatives of *e*-, *trans*-4-, and *trans*-2-$C_{60}dhn_2$ as an electron-acceptor material show the highest output solar cells parameters (power conversion efficiency PCE, open circuit voltage V_{OC}, filling factor, and short-circuit current density) (Figure 17a). These compounds, as we turned out, are characterized by the lowest values of anisotropy (the most thermodynamically favorable structures for *e*-, *trans*-4-, and *trans*-2-$C_{60}dhn_2$ are shown in Figure 18). On the contrary, the devices, utilizing highly anisotropic adducts, show the lowest values of the output parameters (*e.g.*, *trans*-1-$C_{60}dhn_2$). Slight discrepancy of data for *cis*-2- and *cis*-3-bisadducts with the discussed relationship can be explained by the fact that their mixture was used in devices because of the failed separation.

As known, V_{OC} values can be accurately predicted with the use of LUMO energies of acceptors.[154] However, in the case of $C_{60}dhn_2$, we have found a more precise correlation with the anisotropy values than with LUMO levels.[135] Ordering the donor and acceptor phases is necessary for the transport of charge carriers to the electrodes in solar cells. It would seem that the high anisotropy of polarizability should facilitate the ordering. However, the found correlation is reversed (Figure 17a). Therefore, we have assumed that the role of disorder in the charge transport process should be reconsidered.

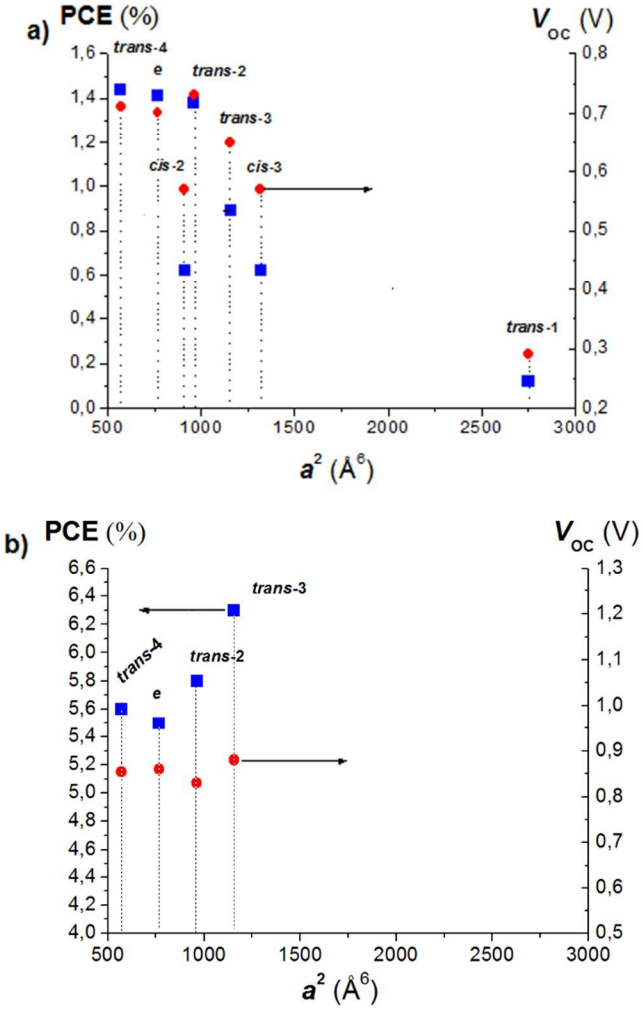

Fig. 17 Correlation between the output parameters of organic solar cells, based on bis(dihydronaphtho)fullerene derivatives, and calculated anisotropies of regioisomeric $C_{60}dhn_2$. Panel a: output parameters PCE and V_{OC} are taken from the experimental work[152] (reprinted with permission from ref 135 © 2013 American Chemical Society). Panel b: output parameters PCE and V_{OC} are taken from the recent experimental work.[155]

Unfortunately, the situation with application of a^2 values to fullerene derivatives for organic solar cells is ambiguous. Very recent experimental work[155] declares the enhanced output

parameters for *trans*-3-C_{60}dhn$_2$. Structurally, the compounds, tested in ref 155, were exactly the same as in the computational case above. We have superposed experimental data on PCE and V_{OC} with anisotropies in Figure 17b. Thus, *trans*-3-C_{60}dhn$_2$ is the most anisotropic among the regioisomers, tested in ref 151. This contradicts to the previous considerations about the enhanced efficiency of the isotropic bisadducts.[135] However, the correlation field of experimental study[155] is narrow (the measured parameters are close to each other) because a half of possible C_{60}dhn$_2$ have not been purified and tested. On the other hand, the calculations[135] did not take into account the alkylcarboxy chains, presented in the compounds from ref 152. Unfortunately, there no other experiments, operating with purified fullerene bisadduts. Thus, the further consideration of anisotropy of polarizability in context of organic solar cells demands additional experimental and theoretical studies.

The examples above, despite of the contradictions, may be important for fullerene photovoltaic applications. Here, we just mention three points of why anisotropy of polarizability matters.

The first deals with the dependence of dielectric permittivity on the polarizability, which is described by Clausius–Mossotti equation (eqn (25)).[14] In the recent study,[156] dielectric constant has been considered as a central parameter for efficient solar cells. The authors use it in a scalar form to find out optimal regimes for photovoltaic devices functioning. Based on our studies on anisotropy of polarizability, we propose that tensorial nature of dielectric permittivity and anisotropy of dielectric permittivity should be taken into account to improve the existing models for assessing the efficiency of organic solar cells.

The second point deals with the polarizability of fullerene charge-transfer complexes, which arise when solar cell works. Polarizabilities of the excited states of such complexes may exceed 2000 Å^3.[60] Standing this, we can assume that the anisotropy of polarizability affects the charge-transfer complexes decay, required for generating the charge carriers.

At last, the role of anisotropy of polarizability may deal with its influence on wetting processes, which we mention in Section 3.4. If de Gennes equation[110] (eqn (23)) is applied to this case, the composite material of organic solar cells may be roughly approximated as nano-droplets of fullerene derivatives (α_L parameter in eqn (23)) wetting the surface of polymer phase (α_S parameter in eqn (23)). This seems reliable in the context of the recent experimental work,[157] in which wetting and surface tension have been efficiently used to explain the observed molecular structure–device function relationship for solar cells utilizing diverse *o*-xylenyl bisadducts of C_{60} as electron acceptor materials.

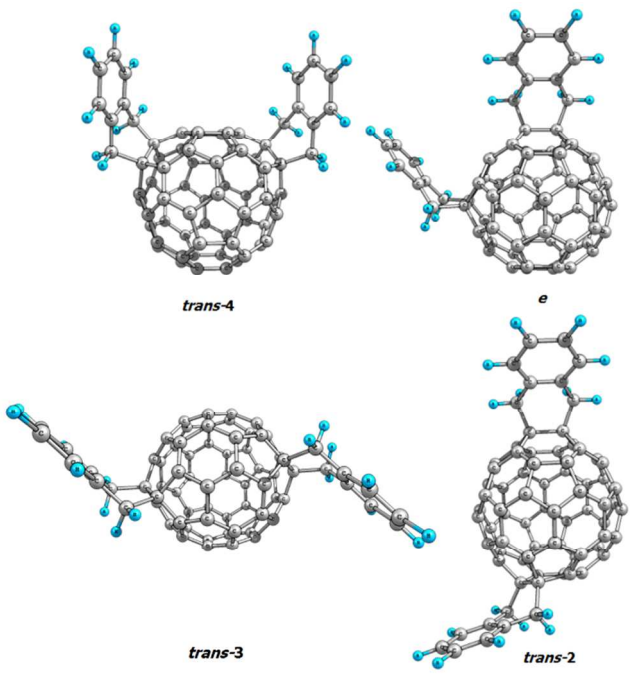

Fig. 18 The most thermodynamically favorable structures for *trans*-4-, *e*-, *trans*-3-, and *trans*-2-C_{60}dhn$_2$.

Finally, we mention another value that may be useful in the field under discussion. This is optical anisotropy, defined as:[29]

$$\delta^2 = \frac{2a^2}{9\alpha^2}. \qquad (40)$$

As it is seen, in the series above, all the bisadducts were isomeric, *i.e.* have the same mean polarizabilities. However, comparing fullerene derivatives with more different structures (*e.g.*, with different nature of addends or their unequal numbers) requires a scaling factor, and eqn (40) provides this.

In the regard of recent application of triscyclopropafullerene derivatives to organic solar cells,[158,159] dependence of anisotropy on the average distance between the addends for 47 possible regioisomers $C_{60}(CH_2)_3$ have been investigated (Figure 19).[135] According to calculations, C_3-symmetry isomer has the lowest anisotropy. This isomer is characterized with equidistance of CH_2 and their uniform distribution on the fullerene core. Additionally, the isomer of $C_{60}(CH_2)_6$ with uniform distribution of addends has been also found isotropic.[135]

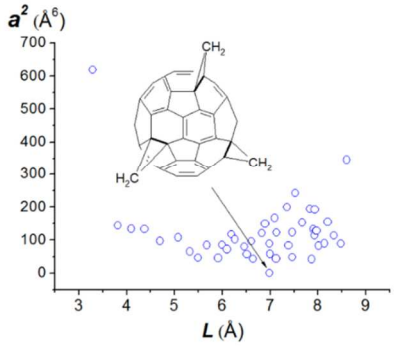

Fig. 19 Dependence of anisotropy a^2 of regioisomeric $C_{60}(CH_2)_3$ on the average distance between the central atoms of addends. The structural formula of the least anisotropic trisadduct is shown. Reprinted with permission from ref 135 © 2013 American Chemical Society

Regardless the application of anisotropy and the physical meaning of the found regularities, anisotropy of polarizability is a good index to describe the structural diversity, emerged upon multiple additions to fullerenes.

4.5 Polarizability and its anisotropy of [60]-PCBM and [70]-PCBM

We separately describe dipole polarizabilities of the substituted cyclopropafullerenes [60]-PCBM and [70]-PCBM because of their high importance for fullerene-based organic photovoltaics.[160] Previously, we have calculated mean polarizability of [60]-PCBM by the PBE/3ζ method (Table 3).[8] For this review, we have used the same computational methodology to compare polarizability of [60]-PCBM and its isomers in the context of the latest studies. As known, [60]-PCBM has 5.6-open isomer[161] and the isomer iso-PCBM with more different structure, which is formed when [60]-PCBM is heated as discovered very recently[139] (its structural formula is shown in Table 3). Moreover, the last one can play important role in the functioning of PCBM-based organic solar cells because it should accompany "traditional" [60]-PCBM in significant amounts. Thus, [60]-PCBM, open [60]-PCBM, and iso-PCBM have almost the same mean polarizabilities (108.4, 108.9, and 109.0 Å^3) despite the differences in their structures. [60]-PCBM shows the lowest anisotropy of polarizability than open [60]-PCBM and iso-PCBM (736.08 *versus* 790.24 and 873.70 Å^6).

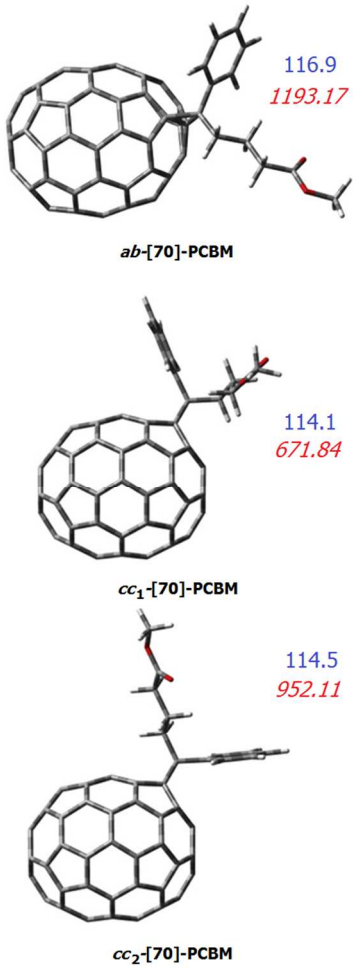

Fig. 20 [70]-PCBM isomers, their mean polarizabilities (in Å^3, blue numbers) and anisotropies a^2 (in Å^6, red numbers), calculated by B3LYP/6-311G(d,p). Adapted with permission from ref 137 © 2014 Elsevier

As is known, the synthesized [70]-PCBM is a mixture of chiral (*ab*-[70]-PCBM) and achiral isomers (cc_1- and cc_2-[70]-PCBM) (Figure 20).[162] Their polarizabilities and anisotropies have been recently calculated by the B3LYP/6-311G(d,p) method in terms of finite-field approach.[137] Calculations show that cc_1-[70]-PCBM and *ab*-[70]-PCBM are the least and the most anisotropic isomers in this set.

In addition, we should mention the recent theoretical work that compares molecular characteristics of [70]-PCBM and its 5.6-open isomer.[136] The work reports the mean polarizabilities for this species 106.5 and 107.2 Å^3, respectively (calculated by CAM-B3LYP/6-31G(d,p)). The C_{70} fullerene has unequivalent bonds in its structure, so several closed and open isomers of [70]-PCBM may exist. Unfortunately, the authors did not clearly indicate what isomers they theoretically investigated in the work.[136] Nevertheless, their computational data agrees with the general trend of higher polarizability for 5.6-open fullerene species.

5 Polarizability of fullerene dimers and oligomers

5.1. Polarizability of C_{60} [2+2]-dimers and oligomers

Fullerene dimers and oligomers are an interesting class of fullerene derivatives that contain two or several cores in the molecules. Due to this structural peculiarity, we have reviewed these compounds separately. Nowadays, many types of such derivatives are known.[163] Among them, [2+2]- and [1+1]-dimers of C_{60} and C_{70} are the most studied. Fullerene [2+2]-dimers (and oligomers) attract also attention due to the closest placement of fullerene cores in a molecule. In addition, these are rigid compounds that can play role of all-carbon building blocks for nanoarchitecture (See refs 164, 165, and references therein). Molecular constructions with four C_{60} fullerene moieties, capable to move like wheels, have been tested as the thermally-driven nanocars.[166] The less-stable [1+1]-dimers can produce fullerenyl radicals (reversibly or irreversibly), which are used for generation of radicals in fullerene-containing systems (see, *e.g.*, ref 167).

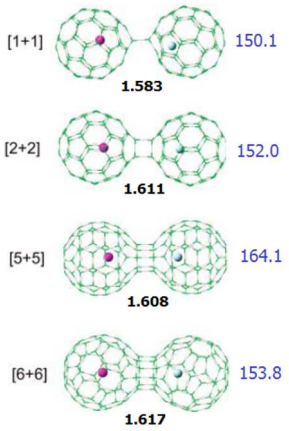

Fig. 21 Mean polarizabilities (in Å^3, blue numbers) and intercage distances (in Å, black numbers) of [Na@C_{60}][F@C_{60}] dimers, calculated at CAM-B3LYP level. Adapted with permission from ref 11 © 2010 American Chemical Society

Polarizability and hyperpolarizability of exotic endohedral [Na@C_{60}][F@C_{60}] with different types of the cage connections have been theoretically studied by Ma *et al.* (Figure 21).[11] However, that work was focused mainly on the hyperpolarizabilities.

Polarizabilities of the following $(C_{60})_n$ [2+2]-oligomers with n up to 5 have been studied by PBE/3ζ method in our studies (Figures 22 and 23).[165] Calculations show that α values of $(C_{60})_n$ are approximately n-fold higher than the polarizability of the pristine fullerene. The obtained values have been analyzed in terms of two additive schemes. Both of them deduce mean polarizabilities of $(C_{60})_n$ the polarizability of the isolated C_{60}. According to the first additive scheme, mean polarizability of $(C_{60})_n$ equals to n-fold C_{60} polarizability:

$$\alpha_{add}^{(I)}\left((C_{60})_n\right) = n\alpha_{C_{60}} \qquad (41)$$

This estimation is rough as far as it does not consider the change of polarizability when several carbon atoms alter the initial hybridization at oligomer forming. The second scheme takes it into account. Accordingly, each of $(C_{60})_n$ molecules is divided into n subunits of two types: one central fullerene core to which the other (n–1) C_{60} fragments are attached. In this case, the additive polarizability equals to

$$\alpha_{add}^{(II)}\left((C_{60})_n\right) = \alpha_{C_{60}} + (n-1)\alpha_{[C_{60}]}, \qquad (42)$$

where $\alpha_{[C_{60}]} = \alpha\left((C_{60})_2\right) - \alpha_{C_{60}} = 97.3$ Å^3 is the increment. It describes the change of polarizability at the addition of one fullerene subunit to the central C_{60} core and the disappearance of π-components of 6.6 bonds in both fullerene cores. Deviations from the schemes

$$\Delta\alpha^{(I)} = \alpha_{DFT} - \alpha_{add}^{(I)}, \qquad (43)$$

$$\Delta\alpha^{(II)} = \alpha_{DFT} - \alpha_{add}^{(II)}, \qquad (44)$$

have been found positive[165] (Figure 24), *i.e.* the exaltation of polarizability occurs when two or several cores present in the molecule. This computational fact was unexpected but reproducible with other DFT[61,165] and long-range corrected DFT techniques.[61] Generally, double bonds in a molecule enhance its mean polarizability. Conversely, polarizability diminishes if π-bonds disappear at chemical transformation without addition of electron-rich chemical groups.[14,29] For example, when two C_{60} molecules are linked resulting in [2+2]-$(C_{60})_2$, two π-bonds cease to exist and, according to the conventional notions, the final polarizability should be lower than the twofold mean polarizability of C_{60}, that is, the deviation from the additive scheme should be negative. However, as follows from the calculated data, $\Delta\alpha^{(I)} > 0$ and the effect increases with n.

For unsaturated hydrocarbons, the analogous exaltation is observed when π-conjugation arises in a molecular system.[66–68] Formation of oligomers results in the increase of the total number of double bonds in a molecule. However, π-electrons do not form an overall system since the subsystems of the conjugated C=C bonds of fullerene units remain isolated at least by three C–C single bonds (two 5.6 bonds of fullerene moiety and one of the cyclobutane fragment). Nevertheless, the subsystems of π-electrons can communicate through space or through σ-bonds, according to the concept of orbital interaction through space.[168] Indeed, the analogous exaltations are observed for the calculated polarizabilities of oligomers $(C_{20})_n$, dimers $(C_{24})_2$, $(C_{30})_2$, $(C_{36})_2$, $(C_{50})_2$, $(C_{70})_2$, and C_{60} adducts with bowl-shaped π-conjugated hydrocarbons (sumanene, hemifullerene, *etc.*).[61,165]

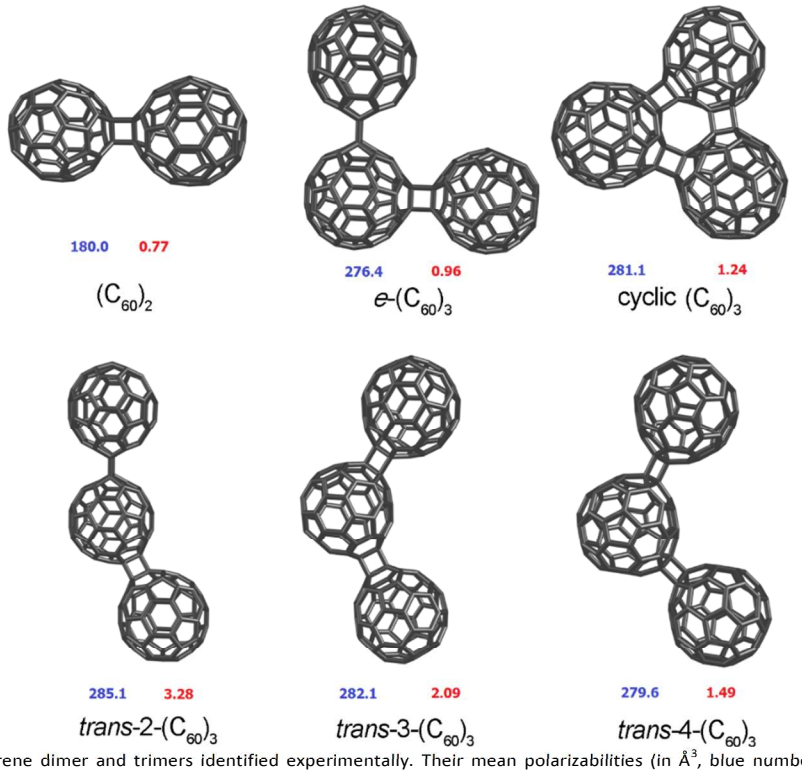

Fig. 22 Structures of the fullerene dimer and trimers identified experimentally. Their mean polarizabilities (in Å^3, blue numbers) and anisotropies (in 10^4 Å^6, red numbers) are shown. Adapted with permission from ref 165 © 2013 Royal Society of Chemistry

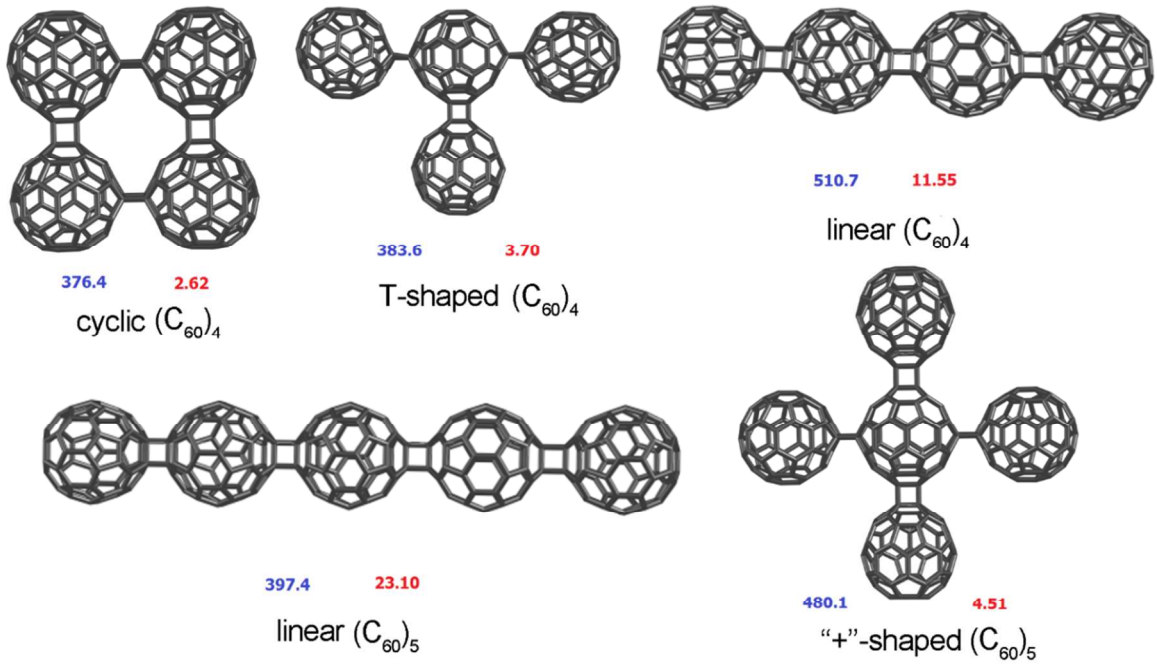

Fig. 23 Structures of the hypothetical fullerene oligomers under study. Their mean polarizabilities (in Å^3, blue numbers) and anisotropies (in 10^4 Å^6, red numbers) are shown. Adapted with permission from ref 165 © 2013 Royal Society of Chemistry

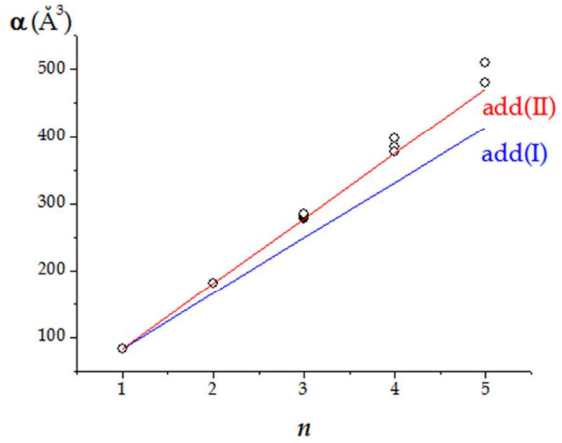

Fig. 24 Dependence of mean polarizability on the number of fullerene cores in $(C_{60})_n$ molecules. Circles correspond to α_{DFT} values; lines present the mean polarizabilities according to the additive schemes. Reprinted with permission from ref 165 © 2013 Royal Society of Chemistry

In the case of $(C_{60})_n$, Δα(II) values linearly increase with the largest distances between the centers of the crosslinked C_{60} cages (L_{max}) (Figure 25). Only $(C_{60})_2$ and cyclic trimer $(C_{60})_3$, both characterized by the smallest intercage distances ($L_{max} \approx$ 9.1 Å), are out the correlation. To explain the physical meaning of the correlation, we have appealed to the basic definitions. Polarizability reflects the molecule's ability to acquire the induced dipole moment in the external electric field (eqn (2)). On the other hand, the magnitude of dipole is proportional to the distance between the centers of positive and negative charges of the molecule.[14,29] Presumably, such centers are induced on the maximally remote atoms in $(C_{60})_n$, so the exaltation increases with the distance between the C_{60} cages. This explains why Δα achieves its highest value for linear nanostructures, having the largest L_{max} values. Note that analogous dependence of Δα (and, consequently α) on the distance between the cages is observed for isomeric $(C_{70})_2$[61] but violated in the case of the endohedrally functionalized dimer [Na@C_{60}][F@C_{60}] (Figure 21).[11]

5.2 Polarizability exaltation of C_{60} dimers: evidence from experimantal studies

Fullerene dimers and, especially, trimers are novel compounds, so the data on their polarizability are absent. In addition, experimental obstacles to its measurement may be due to propensity of $(C_{60})_n$ for decomposition[169] and very low solubility in ordinary solvents.[170] However, correlations between the calculated polarizabilities and observables can be found. As known, the deduction of C_{60} polarizability from the solid-state measurements[171] leads to 89.9 Å^3 that is ~15% larger than the values demonstrated by isolated C_{60} molecules (76.5±8.0 Å^3; molecular beam deflection[38]) or small clusters (79.0±4.0 Å^3; time-of-flight technique[37]). That enhancement has been explained by excitations and charge-transfer between the neighboring C_{60} molecules in a crystal.[171] In the case of C_{60} oligomers, somewhat similar enhancement takes place. Indeed, according to DFT-calculations, the mean polarizability per one cage for $(C_{60})_2$ is ~8.8% higher than the mean polarizability of the isolated C_{60}. Though it is lower than the solid-state effect, there is a significant difference in the experimental and computational situations: unlike to crystalline C_{60}, fullerene cores are chemically bonded in oligomers. Notwithstanding, the similar tendency in both cases allows proposing a common nature of these enhancements caused by the interactions between π-electronic systems of C_{60} cores.

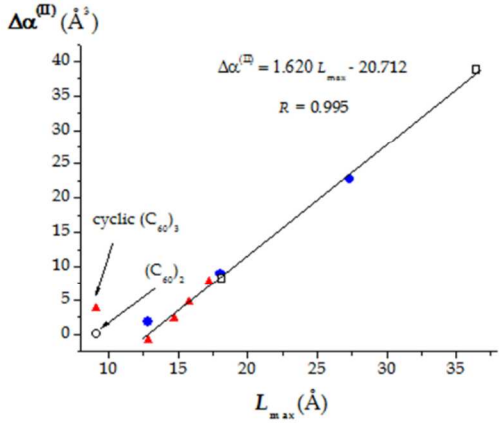

Fig. 25 Dependence of the exaltation of polarizability according to additive scheme II (eqn (43)) on the maximal distance between fullerene units in $(C_{60})_n$ molecules. White circles, red triangles, blue circles, and white squares correspond to oligomers with n = 2, 3, 4, and 5, respectively. The data for $(C_{60})_2$ and cyclic $(C_{60})_3$ have not been included in the correlation. Reprinted with permission from ref 165 © 2013 Royal Society of Chemistry

Recent advances in application of polarizability to chemical reactions[172–174] provide another way to find a correlation between the calculated exaltations and the observed chemical properties of $(C_{60})_2$ and $(C_{60})_3$. For example, the simplest decomposition reactions $A_mB_n\ldots C_p \rightarrow mA + nB + \ldots + pC$ are described by the following change in polarizability $\Delta\alpha_R$:[174]

$$\Delta\alpha_R = m\alpha_A + n\alpha_B + \ldots + p\alpha_C - \alpha_{A_mB_n\ldots C_p} \qquad (45)$$

Moreover, linear correlations between the heat effects of the mentioned reactions and $\Delta\alpha_R$ values have been found, as well as the minimum polarizability principle which states that thermodynamically more stable isomers are characterized by lower $\Delta\alpha_R$ values[173,174] (however, there are compounds that violate this principle[175]). As known, fullerene dimer $(C_{60})_2$ and its derivatives are unstable under the thermal treatment.[163,169] The deviation of polarizability from the additive scheme I and $\Delta\alpha_R$ of the dimer decomposition $(C_{60})_2 \rightarrow 2C_{60}$ are in a simple relation:

$$\Delta\alpha_R = -\Delta\alpha^{(I)}, \qquad (46)$$

that is, the calculated exaltations should reflect the stability of the studied compounds. Therefore, $\Delta\alpha$(I) values of $(C_{60})_2$ and its two derivatives have been compared with available experimental data (Table 3). We have used the results of the experimental studies[176,177] on the formation/decomposition of two auxiliary compounds $[C_{60}(CR_2)_5]_2$ and $C_{60}(C_{60}F_{16})$ (Figure 26). The exaltations of $[C_{60}(CH_2)_5]_2$ and $C_{60}(C_{60}F_{16})$ are approximately equal (12.9 and 12.5 Å^3, respectively) and lower than $\Delta\alpha^{(I)}((C_{60})_2)$ = 14.6 Å^3. It correlates well with the higher stability, observed experimentally for $C_{60}(C_{60}F_{16})$[177] and carboxy-derivative of $[C_{60}(CH_2)_5]_2$.[176]

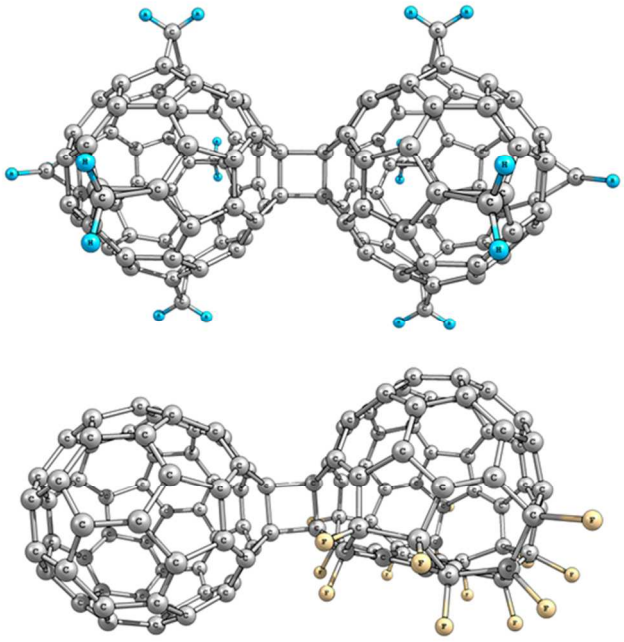

Fig. 26 Structures of dimers $[C_{60}(CH_2)_5]_2$ (top) and $C_{60}(C_{60}F_{16})$ (bottom). Reprinted with permission from ref 165 © 2013 Royal Society of Chemistry

Comparison of $\Delta\alpha^{(I)}$ values of $(C_{60})_2$ and trimers (14.6 against 28.3–37.0 Å^3) predicts that the more polarizable trimers should be less stable. Indeed, the total yield of isomeric trimers is almost ten times lower than the yield of $(C_{60})_2$.[170] Moreover, the exaltation increases in the series *e*-$(C_{60})_3$ < *trans*-4-$(C_{60})_3$ < *trans*-3-$(C_{60})_3$ < *trans*-2-$(C_{60})_3$ that is inversely correlated with the measured content of isomeric $(C_{60})_3$ in the experimentally obtained $(C_{60})_3$ fraction (Figure 7). Thus, the exaltation correlates with the stability of fullerene trimers. Extrapolating this approach, we can make a reasonable prognosis of the increasing instability of the highest oligomers, especially, having linear structure. It can explain, for example, why linear *trans*-1-$(C_{60})_3$ with the maximally distant cages, which seems to have no steric hindrances at its formation, has not been detected in the mixture of synthesized $(C_{60})_3$.[170] However, such structures may become synthetically achievable if fullerene cores are functionalized that results in the wastage of their π-electronic systems and, as consequence, in higher stability (similar to $C_{60}(C_{60}F_{16})$ and $[C_{60}(CR_2)_5]_2$ in comparison with $(C_{60})_2$).

The most significant enhancement of mean polarizability is observed in the case of many-cage fullerene-based molecules with the maximally remote C_{60}.[161] Unfortunately, this also makes the molecules less stable. The linear correlation found may be a landmark for rational design of fullerene-based nanostructures with adjustable response to electric fields. Currently, it seems to be the only way to estimate mean polarizability of the C_{60} fullerene linear polymers with analogous structure (such polymers have been synthesized and recommended as nanofuses; at the same time the fragility of $(C_{60})_n$ has been noted[178]).

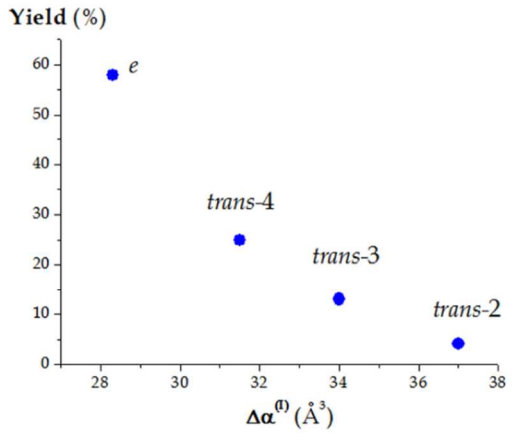

Fig. 27 The calculated exaltations of polarizability *versus* the measured yields of the isomeric fullerene trimers $(C_{60})_3$. Experimental data are taken from ref 170. Reprinted with permission from ref 165 © 2013 Royal Society of Chemistry

Table 8 Mean polarizability α, additive polarizability α_{add}, and its deviation from the additive scheme Δα for 1,4,1′,4′-XC_{60}–C_{60}X dimers (in Å^3; PBE/3ζ calculations). Reprinted with permission from ref 179 © 2013 American Chemical Society.

Dimer	α	α_{add} [a]	Δα
^{t}BuC$_{60}$–C$_{60}$^{t}Bu	197.57	2 × 93.63	10.31
^{t}BuOC$_{60}$–C$_{60}$O^{t}Bu	199.56	2 × 95.37	8.82
^{t}BuOOC$_{60}$–C$_{60}$OO^{t}Bu	202.36	2 × 96.96	8.44
Ph(CH$_3$)$_2$CC$_{60}$–C$_{60}$C(CH$_3$)$_2$Ph	216.92	2 × 102.77	11.38
Ph(CH$_3$)$_2$COC$_{60}$–C$_{60}$OC(CH$_3$)$_2$Ph	214.74	2 × 104.48	5.78
Ph(CH$_3$)$_2$COOC$_{60}$–C$_{60}$OOC(CH$_3$)$_2$Ph	218.79	2 × 105.33	8.13

[a] Twofold polarizability of the respective fullerenyl radical.

5.3 Polarizability exaltation of other fullerene dimers

More recently, the phenomenon of polarizability exaltation has been theoretically found for [2+2]-dimers of other fullerenes with different structure $(C_{20})_2$, $(C_{24})_2$, $(C_{30})_2$, $(C_{36})_2$, $(C_{50})_2$, $(C_{70})_2$ (Figure 28)[61] as well as for C_{60} [1+1]-dimers (Table 8),[179] which are formed in radical reactions of C_{60}. Therefore, the exaltation of polarizability can be considered as a common property of fullerenes family, regardless the type of fullerene cages in a molecules and type of their connection.

6. Insights into molecular switch from fullerene polarizability

Molecular switch is a widespread concept in molecular machinery. It consists in the ability of a molecular system to exist in two or more stable states, differing by any physical property.[180] Fullerene derivatives have become very attractive for switchable molecular devices due to their unique structural and electronic properties.[181–182] Recently, we have briefly overviewed the synthesized and tested fullerene-based switches to recognize what novel fullerene derivatives may be useful for this application.[9] In this context, we have paid attention to their polarizabilities, calculated in our previous works.

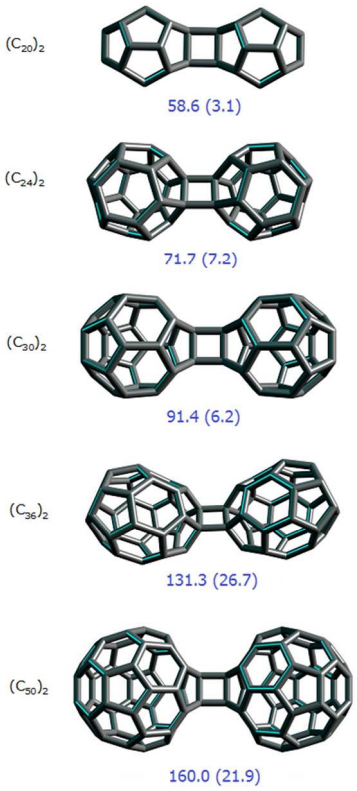

Fig. 28 Structures of hypothetical fullerene dimers. Their mean polarizabilities and polarizability exaltations (in parentheses) are shown in Å^3 (PBE/3ζ calculations). Adapted with permission from ref 61 © 2013 Royal Society of Chemistry

Polarizability is very informative physical quantity and it is sensitive even to small changes in chemical structure of a molecular system.[15] However, it is hard to use it directly to monitor switching in the bistable molecular systems because its measurements usually require a complicated methodology. Meanwhile, polarizability defines other quantities that could be (easily) measured such as refractivity indices, ion mobility, and dielectric constant.[14] Therefore, it can be useful for screening potential compounds for molecular switch because the difference in polarizabilities of two states of molecular switch (split polarizability) may lead to the difference in their polarizability-dependent properties. We have selected three types of the fullerene-based molecular systems that may be considered for the application as molecular switches. These are 1) pairs of isomeric 6.6-closed and 5.6-open fullerene adducts; 2) fullerene dimers with flexible bridge between the cages; and 3) singly bonded fullerene dimers (The systems are listed in order of the increasing split of mean polarizability).[9]

Pairs of isomeric 6.6-closed and 5.6-open fullerene adducts (Figure 4). It is well-known that [2+1]-addition to C_{60} and C_{70} results in at least two types of adducts, *viz*. 6.6-closed (addition to 6.6 bond) and 5.6-open (addition to 5.6 bond with its simultaneous cleavage).[89,140] The preliminary examination of 6.6-closed *versus* 5.6-open fullerene adducts allows pointing out the minimal difference in their nuclear frameworks. It means that these compounds should be almost isoenergetic though 5.6-open species are less stable and isomerized to their 6.6-closed counterparts.[89,140] Meanwhile, the electronic structures of the mentioned compounds differ significantly. The π-electronic system of the parent fullerene remains almost intact in 5.6-closed fullerene adducts whereas it loses one π-bond when the 6.6-closed adduct is formed. As we have shown in our previous theoretical works, mean polarizability reflects the last fact.[8,131] Indeed, 5.6-open adducts, due to the richer π-electronic systems, have mean polarizabilities, which slightly higher than the respective values of the 6.6-closed isomers (Table 4).[8,131]

The difference in mean polarizabilities (Δα split) may be increased if several addends are attached to the fullerene core.[9] Such a structure can be useful for molecular switch if it remains propensity for isomerization. Quantum-chemical calculations show that difference in 4–5 Å^3 is achieved in the case of $C_{60}X_6$ multiadducts with simple X (Table 4). Unfortunately, these are also small values, so another opportunity should be considered to enhance Δα split, for example, varying X moiety to obtain such a pair of monoadducts that would demonstrate a desirably high split.

Another obstacle to creation of the molecular switch, based on the described possibilities, is caused by the irreversibility the reaction in Figure 4; *i.e.* in the most cases, the 6.6-closed fullerene adducts are much more thermodynamically stable than their 5.6-open counterparts. However, this problem seems to be solvable due to the recently demonstrated conversion of the 6.6-closed fullerene adducts into 5.6-open derivatives.[183] Thus, the systems under discussion can be recommended to test their switching, though with reservations.

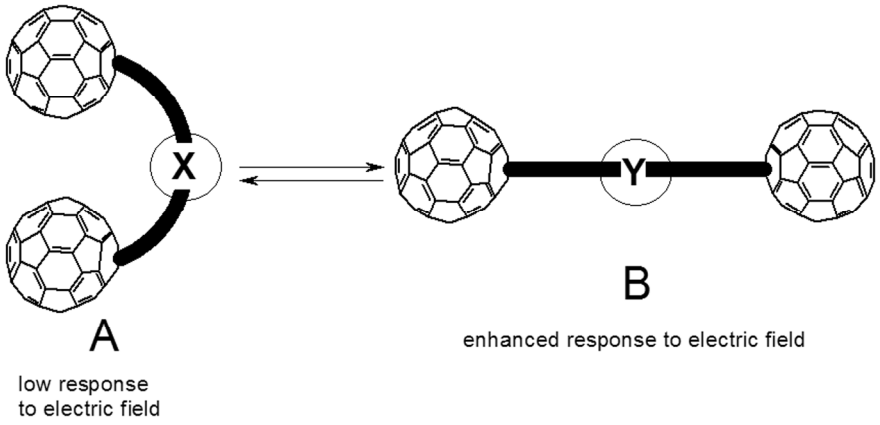

Fig. 29 Hypothetical bicage fullerene-containing system existing in to states characterized with lower (A) and enhanced (B) response to external electric field. Reprinted with permission from ref 165 © 2013 Royal Society of Chemistry

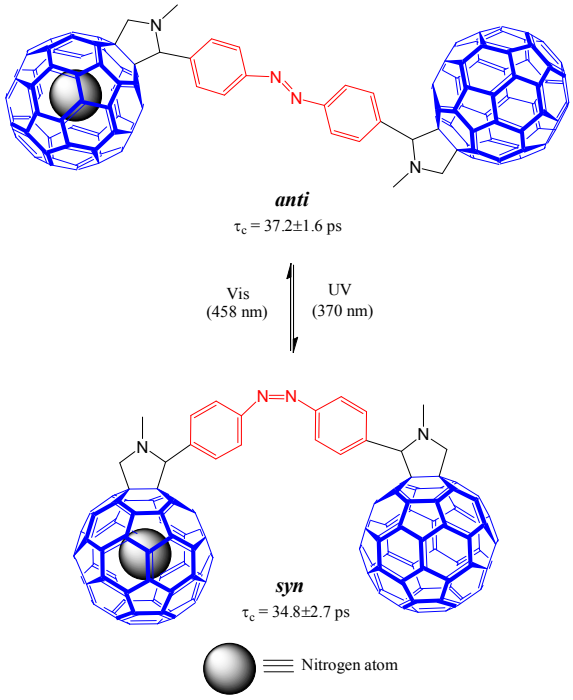

Fig. 30 Molecular switch based on fullerene bicage derivative with photoactive azobenzene bridge and studied in ref 184.

Molecular switch based on the reversible transitions in bicage fullerene derivatives. Recently, we have performed theoretical studies of diverse fullerene [2+2]-dimers and oligomers and found that resulting mean polarizability of such multicage structures depends on the maximal remoteness of the cages.[61,165] Unfortunately, such oligomers are rigid compounds with no transitions between the forms with the closest and the remotest locations of the fullerene cages. However, we have also shown that the described split polarizability may be typical for bicage structures regardless of the type of bridging (for both [2+2]- and [1+1]-dimers[179]).

Therefore, we assume a bicage fullerene system with the cores, connected by a flexible bridge (Figure 29).[165] The initial state of the system A is characterized by a short distance between the fullerene cores. If the bridge undergoes a transformation that increases its linear size (*e.g.*, the well-known photo-induced isomerization or conformational change), the system enters state B with a greater remoteness of the fullerene fragments (Figure 29). In the second state, the molecular system obtains the higher polarizability and, consequently, the enhanced response to an external electric impact. In contrast to state A, it can be facilely manipulated by the external electric field.

The dimer, very similar to the described above, has been previously tested (Figure 30).[184] In the experiments, one of the fullerene cages hosts a nitrogen atom that is decisive for functioning of the dimer as a molecular switch. Its two forms are distinguishable by EPR measurements due to the unpaired electrons of the encapsulated atom. The authors[184] have studied EPR signals of *syn*- and *anti*-isomers and analyzed electron spin lattice and spin-spin relaxation times. Indeed, the molecular rotational correlation time τ_c, deduced from pulse EPR measurements in degassed CS_2, is slightly longer for *anti*-form of fullerene dimer compared to its *syn*-form. The authors explain different EPR behavior of the compound in its *syn*- and *anti*-forms with the changing distance from the nitrogen center of the unpaired electrons and the empty cage (it is more distant in *anti*-isomer, so the influence on its EPR characteristics is weaker).

Additionally, we have found that such a split also depends on the number of double bonds of the subunits in the dimer molecules.[165] Theoretically, if the number of double bonds is larger than 30 (their number in the C_{60} molecule), one should expect the strengthening of $\Delta\alpha$. Thus, the replacement in a fullerene dimer of one of the C_{60} cages by a moiety with a rich

π-electronic system should also demonstrate the split. The list of potential species for such enhancement contains compounds with conjugated double bonds, *e.g.*, porphyrins, polycyclic aromatic hydrocarbons, higher fullerenes and carbon nanotubes. Additional opportunities may arise when carbon nanotubes are used as a part of fullerene-containing molecular switch because the electron-transfer processes between C_{60} and nanotubes strongly depend on the type of the last one.[185]

Molecular switch, based on the reversible dissociation of bicage fullerene derivatives. The reaction of dimerization of fullerenyl radicals $XC_{60}^{\bullet}$ is well-studied.[186] It results in the singly bonded fullerene dimers XC_{60}–$C_{60}X$ (so-called [1+1]-dimers):

$$XC_{60}–C_{60}X \leftrightarrow XC_{60}^{\bullet} \quad (47)$$

Theoretical studies predict that C_{60} singly bonded dimers should demonstrate outstandingly high values of the first[175] and the second[11] polarizabilities. It makes these chemicals prospective for optical applications and nanodevices.

Reversible reaction (46) can change its direction depending the conditions. EPR spectrometry is the easiest way to monitor in what state, dimer or radical, the system is. Additionally, according to our DFT study,[179] the mean polarizabilities of XC_{60}–$C_{60}X$ are more than twice higher compared to those of the respective fullerenyl radicals. It means that the switchable system should be more facilely manipulated by external electric fields when it is in the dimer state. The possible disadvantage of this molecular system is that one of its states has unpaired electron. This may involve $XC_{60}^{\bullet}$ in side processes. However, as shown in experimental and theoretical works, fullerenyl radicals $XC_{60}^{\bullet}$ slowly react with other species, *e.g.*, with molecular oxygen.[179,187,188]

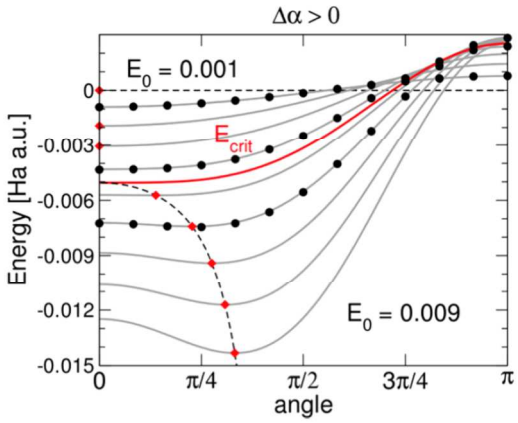

Fig. 31 Model prediction for the total energy of coronene $C_{20}H_{10}$ as a function of the molecule orientation with respect to external electric field. The curve corresponding to the critical field is shown in red. Red points designate thee positions of energy minima. Reprinted with permission from ref 190 © 2013 American Chemical Society

It is noteworthy that systems, such as described, attract attention in another way. Thus, in a solid-state study,[189] it has been shown that thermolysis of the solid fullerene dimers results in both reversible and irreversible generation of radicals $XC_{60}^{\bullet}$ (X = $–CH_2Si(CH_3)_2C_6H_4OCH_2CH(C_2H_5)(C_4H_9)$). The free radicals, irreversibly generated after the first cooling of the solid, do not recombine because of the emergence of a second state of molecular packing, which produces a solid containing a long-lived radical. This free radical acts as a dopant for the fullerene solid and increases the electron mobility.[189]

The situation above is based on the structural control of the dimers' response in the external electric field. There is another opportunity of the use of such highly-polarizable structures for molecular devices. It deals with the reversed influence when the structure of the compound with flexible moieties (capable for conformational transits) is affected by the electric field. This case has been theoretically studied on the example of the bowl-shaped hydrocarbons,[190] which are considered as fullerene precursor. Such hydrocarbons (*e.g.*, coronene $C_{20}H_{10}$, the smallest one) are sufficiently anisotropic: when they interact with the electric field $\boldsymbol{E}$, it is useful to divide their polarizabilities into two parts, parallel ($\alpha_{\parallel}$) and orthogonal ($\alpha_{\perp}$) to the field applied. The authors[186] have analyzed the energy gain ΔU_{tot} of bowl-shaped hydrocarbons in the presence of the field with the intensity E and fixed orientation. In general, it has the following view:

$$\Delta U_{tot} = -E\left(\mu_0 \cos\vartheta + \frac{1}{2}\alpha_{\perp}E - \frac{1}{2}(\alpha_{\perp} - \alpha_{\parallel})E\cos^2\vartheta\right) \quad (48)$$

where, ϑ is the angle of the rotation of a molecule that should move in the field to obtain the equilibium position. For field intensities smaller than a defined critical value E_{crit}:

$$E_{crit} = \frac{\mu_0}{|\alpha_{\perp} - \alpha_{\parallel}|} \quad (49)$$

ϑ = 0 always corresponds to a stable stationary point (minimum) and $\vartheta = \pi$ to an unstable one (maximum). For fields stronger than E_{crit}, a new stationary point appear:

$$\cos\vartheta = \frac{\mu_0}{(\alpha_{\perp} - \alpha_{\parallel})E} \quad (50)$$

The stability of the configuration epends on the difference between $\alpha_{\perp}$ and $\alpha_{\parallel}$: when $\alpha_{\perp} - \alpha_{\parallel} > 0$ it is a minimum and a maximum otherwise. Thus, a new metastable state (existing only if the field applied) may arise (Figure 31). The authors[190] propose the exploiting the response to electric stimulus to tune the molecular orientation. As an example, they quantum-chemically demonstrated it by the structural relaxation of $C_{20}H_{10}$ molecule linked to a (5,5) nanotube fragment (Figure 32).

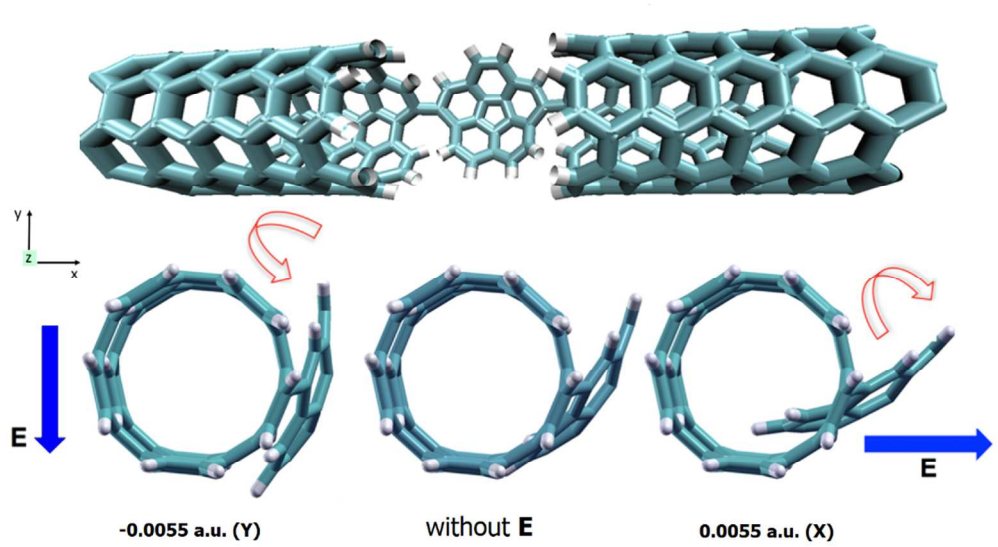

Fig. 32 Field-induced conformational transits, proposed for molecular junctions. Reprinted with permission from ref 190 © 2013 American Chemical Society

Table 9 Mean polarizabilities of noble gas endofullerenes (the respective depression of polarizability, calculated according to eqn (52), are shown in parentheses; mean polarizability of C_{60}, calculated by the same methods, is given for comparison). All values are in Å^3

Endofullerene	Mean polarizability α (depression of polarizability Δα)				
	B3LYP/aug-cc-pV*n*Z[a]	SVMN/aug-cc-pV*n*Z[a]	PBE/aug-cc-pV*n*Z[a]	PBE/3ζ[b]	M06-2X[c]
He@C_{60}	82.0 (–0.2)	82.7 (–0.4)	83.1 (–0.2)	82.6 (–0.1)	78.5 (–0.1)
Ne@C_{60}	82.0 (–0.3)	82.9 (–0.3)	83.1 (–0.4)	82.6 (–0.3)	–
Ar@C_{60}	82.2 (–1.3)	83.1 (–1.5)	83.3 (–1.4)	82.9 (–1.0)	78.8 (–1.2)
Kr@C_{60}	82.4 (–2.1)	83.2 (–2.2)	83.4 (–2.2)	83.0 (–1.4)	–
Xe@C_{60}	–	–	–	83.0 (–2.6)	–
C_{60}	81.9	82.8	83.1	82.7	78.4

[a] *n* = D and T for C and noble gas atoms, respectively. The data are extracted from ref 205. [b] The data taken from ref 206. [c] Basis sets used: 6-31+G(d,p) was applied to C atoms; MG3 basis was applied to He and Ar. The data are extracted from ref 55.

Table 10 Polarizability, its depression, and screening coefficients of the encapsulated molecules, calculated by eqns (51) and (52), respectively

X@C_{60}	α, Å^3	α_X, Å^3	–Δα, Å^3	*c*	Method & reference
H_2O@C_{60}	82.8	1.1	1.0	0.91	PBE/3ζ[209]
H_2O@C_{60}	77.4	0.2	0.05	0.22	BPW91/6-311+G(d)//BPW91/D95V[214]
NH_3@C_{60}	82.9	1.7	1.5	0.88	PBE/3ζ[208]
NH_3@C_{60}	77.6	1.4	1.1	0.77	BPW91/6-311+G(d)//BPW91/D95V[214]
CH_4@C_{60}	83.0	2.3	2.0	0.87	PBE/3ζ[208]
CH_4@C_{60}	78.7	2.0	1.7	0.85	M06-2X/6-31+G(d,p)[55]
CH_4@C_{60}	77.8	1.8	1.2	0.69	BPW91/6-311+G(d)//BPW91/D95V[214]
SiH_4@C_{60}	83.7	4.6	3.6	0.78	PBE/3ζ[208]
CF_4@C_{60}	78.7	2.4	2.1	0.88	M06-2X/6-31+G(d,p)[55]
CO@C_{60}	78.7	1.7	1.4	0.82	M06-2X/6-31+G(d,p)[55]
HF@C_{60}	77.4	0.1	0.01	0.09	BPW91/6-311+G(d)//BPW91/D95V[214]
NHe@C_{60}	82.9	0.8	1.2	1.43	PBE/3ζ[212]
NHe@C_{60}	67.5	0.6	0.8	1.33	M06-2X/6-31G(d)[212]

7. Endofullerene polarizability

Fullerene molecules have empty space inside. This fact was immediately used to put atoms and molecules into their cages that result in endofullerenes (or endohedral complexes), a new class of topological compounds promising for wide-range applications such as radiofarmaceuticals, quantum bits, or photoswitchable devices.[191–193] Such encapsulation may change molecular properties of both the host fullerene and the guest atom/molecule. As consequence, this causes changes in exoherdal reactivity of the fullerene moieties of such

complexes[194–197] as well as the measurable physicochemical properties of the atoms trapped.[193,194,198]

Currently, endofullerene polarizability has been studied only by theoretical methods. In the review, we discuss it starting with the simplest endofullerenes and moving to the more complex species. The chosen order does not reflect chronology of these studies. Indeed, analysis of periodicals shows that studies on endofullerenes started with theoretical treatment of $Sc_n@C_m$ polarizabilities in Torrens's works.[199–200] In 2007, a monopole-dipole interaction approach was applied to study dielectric properties of giant multi-shell carbon nano-onions[202–204] and then double-shell $C_{60}@C_{240}$ nano-onion was studied by DFT in Zope's work.[48] Later, polarizabilities of endofullerenes with encapsulated noble gas atoms,[205–207] simple molecules (H_2O or CH_4),[55,208,209] and relatively large hydrocarbons (norbornadiene and quadricyclane)[57] were calculated.

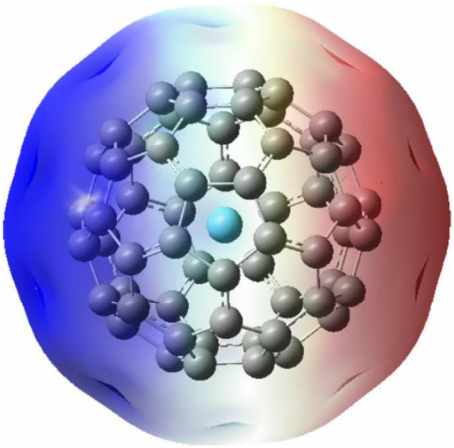

Fig. 33 B3LYP/aug-cc-pVDZ calculated electrostatic potential surfaces of $Ar@C_{60}$ under external field of 0.001 a.u. The blue and red surfaces represent the positive and the negative parts the electrostatic potential, respectively. Reprinted with permission from ref 205 © 2008 Elsevier

Polarizability of the most known endofullerenes with noble gas atoms inside $Ng@C_{60}$ Ng = He–Kr has been exhaustively studied with several DFT methods.[55,205–207] Being intrinsically non-polar, these species obtain induced dipole moments in the presence of the external field. The induction of the dipole is clearly demonstrated by the electrostatic potential (Figure 33). Though noble gases have the saturated electronic shells and C_{60} has enough empty space inside to avoid interactions between the C_{60} cage and the trapped atoms, mean polarizabilities of $Ng@C_{60}$ do not equal to the sum of the contributions α_{Ng} and $\alpha_{C_{60}}$ (Table 9). This was first found by Yan *et al.*[205] and later in our work.[206] Yan *et al.*[205] analyzed such a decrease in polarizability in terms of decomposing the polarizability of a molecular system into site-specific contributions (the details of this approach are discussed in ref 210). For this purpose, the polarizability of each $Ng@C_{60}$ has been partitioned as:

$$\alpha_{Ng@C_{60}} = \alpha^{P}_{C_{60}} + \alpha^{Q}_{C_{60}} + \alpha^{P}_{Ng} + \alpha^{Q}_{Ng} \qquad (51)$$

where P and Q denote local atomic and charge-transfer contributions, respectively. The values of $\alpha^{P}_{C_{60}}$ have been found very close to those of the pristine C_{60} whereas $\alpha^{Q}_{C_{60}}$ increases slightly from He to Kr. On the contrary, the local polarizabilities α^{P}_{Ng} increase from He to Kr and α^{Q}_{Ng} remains null. However, this scheme does not definitely explain why polarizabilities of the encapsulated noble gases are lower than polarizabilities of the respective free atoms.

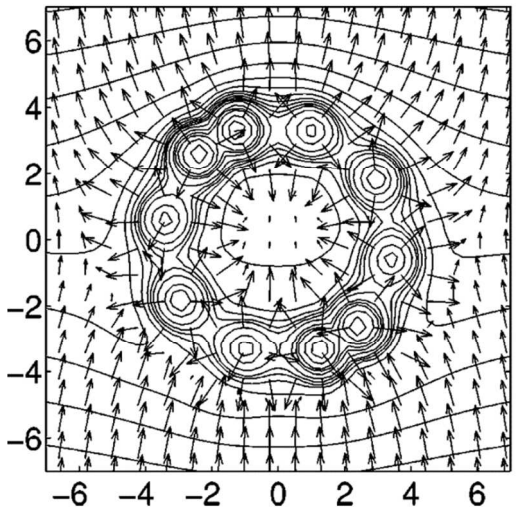

Fig. 34 Equipotentials and field vectors of $\Delta\boldsymbol{E}$ on the cut plane. The vertical direction is the C_5 axis, along which a field of 8.23 V nm^{-1} is applied, and values of the axis are in Å. There are strong fields near the atoms; for clarity, field vectors longer than 10 V nm^{-1} were reduced to this length. Reprinted with permission from ref 211 © 2004 American Institute of Physics

Delaney and Greer have studied screening effects taking into account interaction of the hollow C_{60} with the electric field.[211] The C_{60} fullerene has rich π-electronic system that generates its own electric field. This intrinsic field makes an obstacle for penetration for the external one (Figure 34). Indeed, according to the estimations,[207] only ~25% of the external field penetrate the interior of the C_{60} fullerene, *i.e.* C_{60} acts as a small Faraday cage. It is reflected on the polarizability of the encapsulated atoms: it becomes smaller compared to the free state.

Later,[206] we have analyzed the screening effects for noble gas endofullerenes with C_{20}, C_{24}, C_{28}, C_{36}, C_{50}, and C_{60} as the cage molecules in terms of the additive schemes considering the deviation:

$$\Delta\alpha = \alpha_{X@C_n} - \left(\alpha_{C_{60}} + \alpha_X\right) \qquad (52)$$

We have found that the deviation Δα can be both positive and negative. In the case of noble gas endofullerenes with C_{36}, C_{50}, and C_{60} cages, $\Delta\alpha < 0$ as in the previous theoretical work.[205] (Table 1) (note that $\Delta\alpha < 0$ is also observed for endohedral complexes of C_{30} and C_{32} fullerenes with noble gases as we have shown in the unpublished data), *i.e.* the depression of polarizability takes place. In the case of the small cages C_{20},

C_{24}, and C_{28}, we have observed the exaltation ($\Delta\alpha > 0$) (Figure 35).

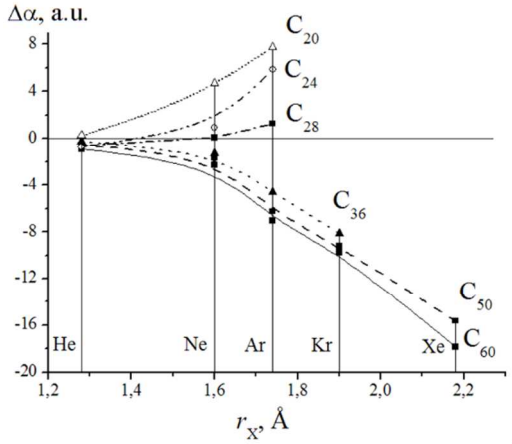

Fig. 35 Polarizability depression of endofullerenes *versus* atomic radii of the encapsulated noble gas atoms. Reprinted with permission from ref 206 © 2010 Springer

Polarizability in classic theory is interpreted as the molecule's electronic cloud. Therefore, we have tried to explain the differences in signs of $\Delta\alpha$ by the compression of electronic clouds. In the general case, the relation between the sizes of the guest atom and the host cavity is decisive for polarizability. We assume that the endoatom induces high pressure on the carbon cage; it "extrudes" electronic density from the inner cavity of the cage and therefore increases the total polarizability of the endohedral complex ($\Delta\alpha > 0$). Another situation likely occurs for larger fullerene. In this case, the pressure of the carbon cage prevails, so the endoatom is compressed and the total polarizability decreases ($\Delta\alpha < 0$). This explanation is too mechanistic and ignores the charge transfer between the guest and the host molecules. Nevertheless, the known compression of metal atoms in endohedral complexes[198] supports our assumption.

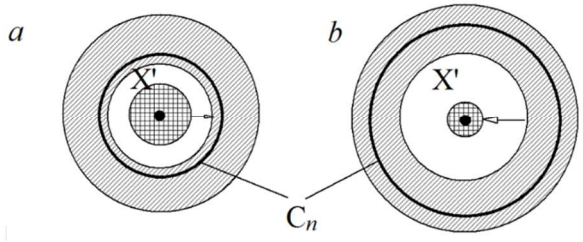

Fig. 36 Polarizability exaltation (a) and depression (b). The first one corresponds to the pressing out the electronic cloud in endofullerenes with less than 30 atoms; the second represents the compression of the endoatom in endofullerenes with more than 30 atoms. Reprinted with permission from ref 206 © 2010 Springer

The model of quenched polarizability, stating that the polarizability of an atom or functional group may significantly vary depending on the environment,[55] also suitable for explanation of the nonadditivities observed for endofullerene polarizability (though it seems less effective for understanding the positive deviations). The resulting polarizability depends on how many space is reserved for the location of the chemical group. Later, in ref 55 and in our works[206,208] the depression of polarizability of endohedral complexes of C_{60} with simple molecules has been stated (Table 2). Thus, this phenomenon is a general trend. As shown within the quenched polarizability model,[55] the fullerene cage does not change its polarizability when it traps atoms/molecules; *i.e.* depression $\Delta\alpha$ is related to the decrease in the polarizability of the guest. Therefore, we have recommended[212] the value

$$c = \frac{|\Delta\alpha|}{\alpha_X} \qquad (53)$$

as a screening coefficient. It lies in the range 0.78–0.91 for most of the studied molecules (Table 10). However, we should mention the found exception when $c > 1$. This is observed for DFT-calculated mean polarizability and its depression for NHe@C_{60} complex.[212] Such a complex has been synthesized recently[213] and contains the N…He inside, which exist in a free state only in specific conditions. Thus, very high depression ($|\Delta\alpha| > \alpha_X$) may be due to the stabilization effect of the fullerene on this complex.

In context of the screening we mention the pnictogen endofullerenes N@C_{60} and P@C_{60}, promising as quantum qubits.[215–217] Their mean polarizabilities and depressions (in parentheses) are 83.3 (–0.3) and 83.2 (–0.83) Å^3, respectively (PBE/3ζ calculations[23]). It is necessary for the quantum processing to manipulate the spin of the endo-atom. At the same time, it would be better if the guest atom remain available for external electric fields that create a harmful interference in the qubit functioning. Polarizability allows numerical estimations how deeply the trapped atom is affected by the external impacts. For example, according to eqn (53), the screening of P atom in P@C_{60} (c = 0.83) is more effective compared to N in N@C_{60} (c = 0.31).[23] The larger depression in the case of P@C_{60} reflects its higher stability compared to N@C_{60} that has been shown in the theoretical study of pnictogen endofullerenes.[218] The mentioned study[218] also predicts that trapped nitrogen atom can be released by the complexation of N@C_{60} with CS_2. This fact is indicated by the relatively low screening coefficient for N@C_{60}.

Exaltation of polarizability takes place in the functionalized fullerenes that has been demonstrated for the Ne@$C_{20}H_n$ fullerene hydrides with n = 2, 6, 12 and 20 by PBE/3ζ and TD-HF/6-31G(d) methods.[207] We have expected the decrease of exaltation but found the non-monotonic dependence of $\Delta\alpha$ on n number (Ne@$C_{20}H_6$ < Ne@$C_{20}H_{20}$ < Ne@C_{20} ≈ Ne@$C_{20}H_{12}$ < Ne@$C_{20}H_2$). As it turned out, $\Delta\alpha$ values well inversely correlate with the covalency factors of the interaction between Ne atom and the most remote carbon atoms of the $C_{20}H_n$ cages.

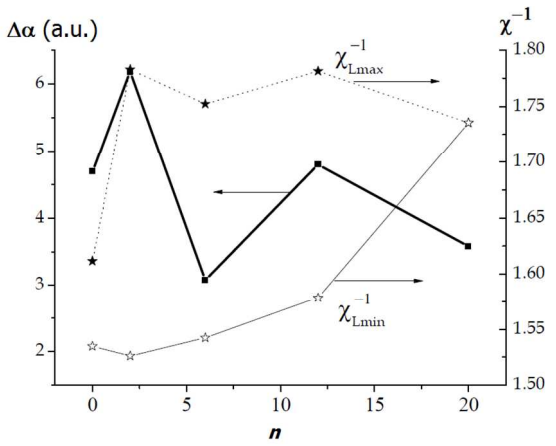

Fig. 37 Dependences of polarizability exaltation of the series of Ne@$C_{20}H_n$ endofullerenes on the reversed covalency factors χ^{-1} that correspond to the maximal (L_{max}) and minimal (L_{min}) internuclear distances between the Ne atom and the cage (PBE/3ζ calculations taken from ref 207).

The described nonadditivities are typical for the other fullerenes and more complex encapsulated molecules (*e.g.*, in the case of the endofullerenes of C_{70}, C_{80}, C_{90}, C_{100}, and C_{120} with the trapped quadricyclane and norbornadiene molecules[57]). The most complex objects, for which depression of polarizability has been postulated, are $C_{60}@C_{240}$ endofullerene (studied by DFT[48]) and multi-shell carbon nano-onions (*e.g.*, $2(C_{540}@C_{960})@C_{2910}$, studied in terms of monopole-dipole interaction approach[202–204]). For $C_{60}@C_{240}$, depression of polarizability and screening coefficient equal to –74.1 Å^3 and 0.90, respectively (PBE/NRLMOL calculations[48]).

However, the list is not limited by the mentioned nanostructures. Depression of polarizability have been observed in computations of metal-silicon clusters,[219] endohedral complexes of silsesquioxanes,[220] boron-nitride fullerene $B_{36}N_{36}$,[57] hollow silicate $Si_{16}O_{24}(OH)_{16}$[57] and even in supramolecular ensembles (*e.g.*, $CH_4@nH_2O$[221]). In addition, polarizabilities of encapsulated fullerene dimers,[11] endometallofullerenes, (*e.g.*, Li@C_{60}[222] and Ti@C_{28}[223]) metal-trinitride endofullerenes,[224] and the structures with both-side functionalization (*e.g.*, Ln@C_{20}-glycine conjugates with Ln = Ce and Dy[225]) have been also theoretically studied. Though these works did not describe the phenomenon of polarizability depression, it obviously takes place. Thus, the influence of confinement on the polarizability is a general property for diverse chemical objects.

In the lists above, we do not include the endohedral complexes of C_{72} and C_{74} fullerenes because their calculations[226,227] have been incorrectly performed (ref 227 provides the unreliably high values for mean polarizability for La@C_{72} and its derivative; ref 226 states zero values for α_{xx} and α_{yy} of the polarizability tensor of Ba@C_{74} and unreliably high α_{zz}).

Mean polarizabilities correlate with chromatographic retention times.[228] Moreover, such a correlation has been found for endometallofullerenes[34] but with the reservation. To estimate retention times, the authors[35] have used polarizabilities of the empty fullerenes instead of the values of the filled ones. We consider that this is possible due to the depression of polarizability.

Unfortunately, there are no theoretical works on the inadditivities of endometallofullerene polarizability though this is rather widespread class of the endohedral species.[194] Based on the reviewed studies, we propose two cases for mean polarizability of endometallofullerenes based on C_{60} and its higher analogues. The absence of covalent bonds or charge transfer between the trapped atom/cluster and the fullerene skeleton (the first case) must lead to the depression of polarizability due to the compression of the guest's electronic cloud. When the covalent bonds or charge transfer arise (the second case), the electronic clouds of the fullerene cage and the guest atoms are united and mean electronic polarizability of endohedral structure is contributed from the polarizabilities of the guest and the host. In addition, the endometallofullerenes in the second case have permanent dipole moments. It means that orientational effects should be taken into account according to eqn (10) when calculating the total polarizability.

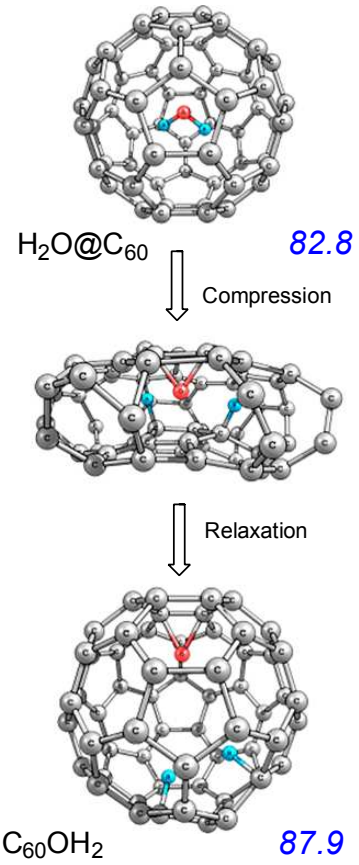

Fig. 38 Evolution of mean polarizability (in Å^3) upon the chemical transformation of water endofullerene (PBE/3ζ calculations taken from ref 209).

Indeed, polarizability of X@C_{60} and accompanied values can provide useful information about in what state the encapsulated species are. For example, in our study of the pressure-induced transformation of $H_2O@C_{60}$,[209] we have theoretically considered the reaction (Figure 38), in which

water dissociates and O and H atoms react with the inner surface of C_{60}. This fact can be monitored by the evolution of polarizability (though the changes are small): depression of polarizability takes place in $H_2O@C_{60}$ but it vanishes in the product of the transformation (Figure 38).

The question about the placement of the trapped atoms inside the fullerene cages is not simple. Anisotropy of polarizability may be useful to assist in uncovering this case. It reflects symmetry (or its absence) in the molecular structure. For example, it has been computationally demonstrated that after encapsulation $H_{20}@C_{80}H_{60}$ and $H_{20}@C_{80}F_{60}$ remain isotropically polarizable ($a^2 = 0$).[229] Thus, despite the significant structural changes, these molecular systems retain the pristine symmetry of the hollow cage.

In the end of this Section, we mention theoretical works in the field of chemical physics of endofullerenes.[230,231] These works approximate the fullerene cages as confining potentials and try to reveal relationships between the electronic structure of the encapsulated hydrogen atom and its polarizability. As shown by this simple case, polarizability presents aspects which are essentially related to the behavior of the wavefunctions.[230] The interesting result has been obtained for the series of multishell endohedral complexes $H@C_{60}$, $H@C_{60}@C_{240}$, and $H@C_{60}@C_{240}@C_{540}$. It is shown that the addition of new walls does not modify the polarizability of the ground state of H atom but changes significantly those of the excited states.[231] However, such a detailed analysis seems to be hardly transferrable to the cases of the more complex endo-atoms.

8. Polarizability of fullerene ions and derivatives with ionic bonds

Fullerenes can generate negative and positive ions (*e.g.*, C_{60}^{z-}, z = 1–6 and C_{60}^{z+}, z = 1–3).[232] The volumes of C_{20}, C_{36}, C_{60}, and C_{70} have been previously studied in comparison with the uncharged states.[233] In all cases, the cage enlarges when both positively and negatively charged. However, this trend (expected from common notions) is not typical for mean polarizability, which has the dimension as volume. When negatively charged, mean polarizability of the C_{60} cage increase according to DFT-calculations (Figure 39). However, in the positive part of the plot, $\alpha(C_{60}^{z+})$ remain almost unchanged up to z = 6 (PBE/3ζ) or grows up very slowly (B3LYP/Λ1) with increasing charge. If electrons leave the cage upon formation of C_{60}^{z+}, one can expect the decrease of polarizability. Possibly, it does not occur due to the cage expansion that makes C–C weaker and, consequently, more polarizable. This compensates the decrease in polarizability, caused by electron loss. The analogous situation has been observed in high-level CCSD/UCCSD computations of unsaturated hydrocarbons and their cations.[234] Except for the smallest members in each series (benzene and butadiene), mean polarizability increases upon ionization (electron removal), and this increase becomes more pronounced with larger molecular size.[234]

This compensation seems impossible when endohedral atoms has the bonds with the internals of the cage. For example, the charged endofullerene with the coordinated Li atom $[Li@C_{60}]^+$ demostrates the lower polarizability than the neutral $Li@C_{60}$, according to the accurate MP2 and DFT calculations.[220]

Fullerene may also form ionic compounds and clusters with metals, which contain ionic bonds in their structure. These derivatives are mainly clusters in their nature. Some of polarizability and electric susceptibility measurements for mixed clusters M_nC_{60} (M is an alkali metal) have been previously reviewed.[15,235] In the present paper, we mention those and focus on a few newer compounds.

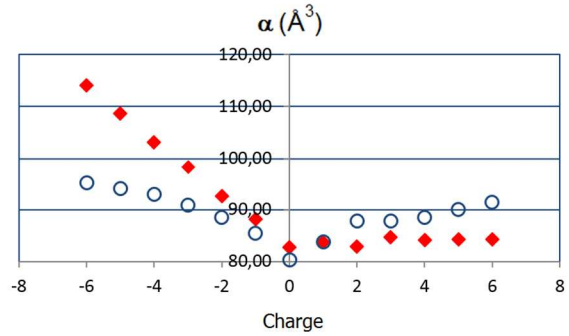

Fig. 39 Dependence of mean polarizability of C_{60} ions on the charge, obtained by PBE/3ζ (red diamonds) and B3LYP/Λ1 methods (white circles).

High dipole moments are typical for most of the C_{60}-alkali metal clusters.[15,236] In the context of the dielectric properties, it means that in measurements of dielectric susceptibility χ one should take into account the orientational polarizability, defined by eqn (10):

$$\chi = \alpha + \frac{\mu_0^2}{3kT} \qquad (54)$$

The measured susceptibilities are of 10^3 Å^3 order of magnitude[15,236–238] The second (orientational) term of eqn (54) is decisive for χ values. It was clearly demonstrated with the reverse temperature dependence for KC_{60} (Figure 40).[237] The authors[237] observed no permanent dipole moment for KC_{60}. This fact and the giant susceptibility allows proposing that KC_{60} has no fixed structure and potassium atom skates on the C_{60} surface.

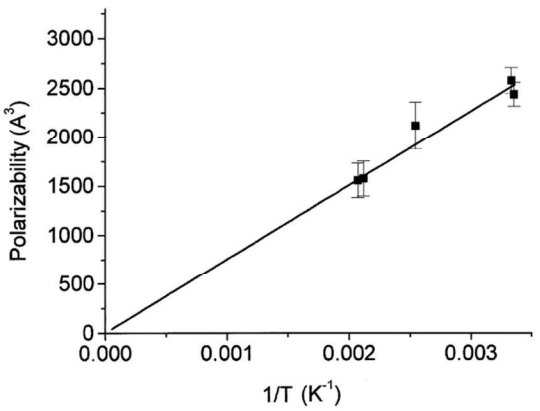

Fig. 40 Temperature dependence of the polarizability of KC_{60}. Line represents the simulation by eqn (54). Reprinted with permission from ref 237 © 2000 The American Physical Society

The molecular analogues of the clusters above K…$C_{20}F_{20}$, K…$C_{60}F_{20}$ (C_{3v}) and K…$C_{60}F_{60}$(C_{6v}) have been theoretically studied (Figure 41).[239] After the DFT-optimization, their mean polarizabilities have been estimated by the HF/6-31+G(d) method: these are 30.0, 100.0, and 94.5 Å^3, respectively. The most interesting in this results is that the oblong carbon nanostructure K…$C_{60}F_{60}$ (C_{6v}) has higher mean polarizability than the compact K…$C_{60}F_{20}$ (C_{3v}) (potassium atom is more remote from the center of the $C_{60}F_{60}$ (C_{6v}) cage). This is reminiscent to the structural dependence of fullerene oligomer polarizability and differs from the case of the exohedral fullerene derivatives with non-fullerene addends.

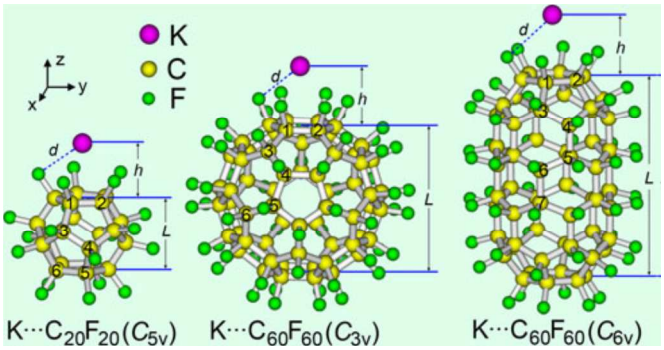

Fig. 41 Optimized geometries of K…perfluorofullerene species (B3LYP/6-31G(d) calculations) Reprinted with permission from ref 239 © 2000 Springer

Another perspective class of ionic fullerene derivatives can arise from fullerenols that are able to form salts with metals.[240] Dielectric properties sodium fullerenol salt have been measured recently.[241] The measured values conductivity and dielectric response of $C_{60}(ONa)_{24}$ were interpreted the results in terms of polarizability. Thus, polarizability of this material is mainly due to the distortion of the ionic bonds. The last ones are tight enough that no ionic contribution in the conductivity is observed up to 550 K. In this work, the reduction of the orientational effects upon increasing temperature has been also observed.[241] This means that $C_{60}(ONa)_{24}$ has a non-zero dipole moment. Based on this statement, we conclude that $C_{60}(ONa)_{24}$ has the non-uniform distribution of C–O$^-$…Na$^+$ bonds on the C_{60} surface. This information is valuable, regarding the lack of the structural information about fullerenols.

9. Conclusion and perspectives

In the review, we have analyzed the results of theoretical and experimental studies of polarizability of different fullerene-containing compounds, trying to cover all the possible classes. Thus, nonadditivity accompanies their polarizability. The negative deviation from the additivity (depression of polarizability) has been found in the case of fullerene exoherdal derivatives with simple addends and endofullerenes with more than 30 carbon atoms in the molecule. The positive one (exaltation of polarizability) is typical for fullerene bi- and multicage derivatives and endohedral derivatives of small fullerenes (C_{20}, C_{24}, and C_{28}). These additivity violations correspond to the conventional additive schemes, so one can find such an additive scheme that will be able to take into account all the effects described. However, the rough schemes, shown in the review, allowed deducing general formula for calculations of mean polarizability of fullerene adducts (eqn (37)) and screening coefficient for encapsulated atoms/molecules for endofullerenes (eqn (53)) as well as correlations between the polarizability of fullerene dimers and the remoteness of fullerene cores in their structure. These should be helpful for the relevant experiments on fullerene derivatives polarizability.

Despite the fact that the discussed data on are mainly computational, these well correlate with the known chemical and physical properties of fullerenes and their derivatives. Moreover, the reviewed data demonstrates that this material is not tacit numbers but very effective tool for understanding of unusual physicochemical processes in fullerene-containing systems and the design of the novel fullerene derivatives with improved molecular and macroscopic properties. Among them, we point insights into fullerene-based molecular switch and fullerene bisadducts for organic solar cells.

Based on the cited papers, we consider that the application of polarizability to fullerene science is in the starting phase. Indeed, its applications are striking but non-numerous. However, we may expect the novel cases, which may arise from the remarkable achievements in the studies of correlations between the polarizability of organic compounds and their interaction with positrons,[242] its use for understanding physicochemical processes in photovoltaic devices,[243,244] fullerene-containing polymers,[245] and biological systems.[246] Polarizability should be taken into account by mechanistic studies, when classic reactions are performed in electric fields.[247] Thus, theoretical studies of polarizability in terms of transition state theory are currently performed.[248]

Endofullerene polarizability provides a universal model for description of screening effects and the confined molecules' behavior under electric fields. This model is easily extrapolated to the more complex encapsulated objects (see, *e.g.*, ref 249) as well as more complex encaging nanostructures.

Another opportunity for this field arise from the applications of carbon nanomaterials. As shown recently, polarizability is sensitive to their mechanical deformations[250] and may be important for understanding of the encapsulated molecules' behavior.[251] In addition, it may provide new insights into the methane[252] and hydrogen[253,254] storage by carbon materials under the external electric fields. Another perspective way to use polarizability deals with moving and trapping nano-objects by laser pulses and electric impacts.[255–257] Obviously, this list can be extended.

The main challenges of application of polarizability originate from the difficulties of its measurements or (in certain cases) accurate calculation. Thus, the polarizability has been used mainly in qualitative aspect for understanding the processes in fullerene-based nanosystems. We hope that the performed review on polarizability of fullerenes and their derivatives will be useful for their further theoretical and especially experimental studies dealing with applications. The title of the review might seem audacious. However, we believe that in recent years it will be justified.

Acknowledgements

The author is grateful to Markus Arndt (University of Vienna, Austria), Ramil G. Bulgakov (Institute of Petrochemistry and Catalysis of RAS, Russia), Eugene Katz (Ben-Gurion University of the Negev, Israel), Sergey L. Khursan (Institute of Organic Chemistry, Ufa Scientific Centre of RAS, Russia), Eiji Ōsawa (Nano Carbon Institute, Japan), Roberto Rivelino (Universidade Federal da Bahia, Brazil), and Ajit J. Thakkar (University of New Brunswick, Canada) for their assistance at the diverse steps of the theoretical study on fullerene polarizability.

In 2009–2014, the Presidium of Russian Academy of Sciences financially supported the author's works on polarizability (Program No 24 "Foundations of Basic Research of Nanotechnologies and Nanomaterials).

Notes and references

Institute of Petrochemistry and Catalysis, Russian Academy of Sciences, 450075 Ufa, Russia. E-mail: diozno@mail.ru; Fax: +7 347 284275.

1. E. Ōsawa, *Kagaku*, 1970, **25**, 854.
2. D. A. Bochvar and E. G. Galpern, *Dokl. Akad. Nauk SSSR*, 1973, **209**, 610.
3. H. W. Kroto, J. R. Heath, S. C. O'Brien, R. F. Curl and R. E. Smalley, *Nature*, 1985, **318**, 162.
4. E. Ōsawa, *Philos. Trans. R. Soc. London, Ser. A*, 1993, **343**, 1.
5. W. Andreoni, *Annual Rev. Phys. Chem.*, 1998, **49**, 405.
6. K. Tokunaga, *Computational Design of New Organic Materials: Properties and Utility of Methylene-Bridged Fullerenes C_{60}*, in *Handbook on Fullerene: Synthesis, Properties and Applications*, ed. R. F. Verner and C. Benvegnu, Nova Publishers, New York, 2013, pp. 517-537.
7. Y. Wang, G. Seifert and H. Hermann, *Phys. Stat. Sol. A*, 2006, *203*, 3868.
8. D. Sh. Sabirov, *Polarizability of C_{60}/C_{70} Fullerene [2+1]- and [1+1]-Adducts: A DFT-Prognosis*, in *Density Functional Theory: Principles, Applications and Analysis*, ed. J. Morin and J. M. Pelletier, Nova Publishers, New York, 2013, pp. 147–170.
9. D. Sh. Sabirov, *Fullerene Derivatives for Molecular Switch: Recent Advances and Theoretical Insights from the Polarizability*, in *Fullerenes: Chemistry, Natural Sources and Technological Applications*, ed. S. B. Ellis, Nova Publishers, New York, 2014.
10. A. G. H. Barbosa and M. A. C. Nascimento, *Chem. Phys. Lett.*, 2001, **343**, 15.
11. F. Ma, Zh.-R. Li, Zh.-J. Zhou, D. Wu, Y. Li, Y.-F. Wang and Z.-Sh. Li, *J. Phys. Chem. C*, 2010, **114**, 11242.
12. L. Jiang, J. Gu and X. Zhu, *J. Mol. Model.*, 2011, **17**, 1041.
13. L.-J. Wang, S.-L. Sun, R.-L. Zhong, Y. Liu, D.-L. Wang, H.-Q. Wu, H.-L. Xu, X.-M. Pan and Z.-M. Su, *RSC Adv.*, 2013, **3**, 13348.
14. K. D. Bonin and V. V. Kresin, *Electric-Dipole Polarizabilities of Atoms, Molecules and Clusters*, World Scientific, 1997.
15. M. Broyer, R. Antoine, E. Benichou, I. Compagnon, Ph. Dugourd and D. Rayane, *C. R. Physique*, 2002, **3**, 301.
16. J. N. Israelachvili, *Intermolecular and Surface Forces*; Academic Press: Amsterdam–Boston–Heidelberg–London–New York–Oxford–Paris–San Diego–San Francisco–Singapore–Sydney–Tokyo, 1991.
17. M. L. Bossi and P. F. Aramendía, *J. Photochem. Photobiol. C: Photochem. Rev.*, 2011, **12**, 154.
18. A. Painelli, F. Terenziani and Z. G. Soos, *Theor. Chem. Acc.* 2007, **117**, 915.
19. H.-J. Schneider, *Angew. Chem.*, 2009, **48**, 3924.
20. P. W. Fowler, P. Lazzeretti and R. Zanasi, *Chem. Phys. Lett.*, 1990, **165**, 79.
21. M. R. Pederson and A. A. Quong, *Phys. Rev. B*, 1992, **46**, 13584.
22. R. Antoine, Ph. Dugourd, D. Rayane, E. Benichou, M. Broyer, F. Chandezon and C. Guet, *J. Chem. Phys.*, 1999, **110**, 9771.
23. D. Sh. Sabirov, A. A. Tukhbatullina and R. G. Bulgakov, International Conference "Advances Carbon Nanostructures", 1−5 July, 2013, St. Petersburg, Russia, p. 52.
24. D. Sh. Sabirov, A. D. Zakirova, A. A. Tukhbatullina and R. G. Bulgakov, 15th International Conference on DFT and Its Applications, 9–13 September, 2013, Durham, UK, p. 176.
25. D. W. Snoke, M. Cardona, S. Sanguinetti and G. Benedek, *Phys. Rev. B*, 1996, **53**, 12641.
26. S. Guha, J. Menéndez, J. B. Page and G. B. Adams, *Phys. Rev. B*, 1996, **53**, 13106.
27. G. K. Gueorguiev, J. M. Pacheco and D. Tománek, *Phys. Rev. Lett.*, 2004, **92**, 215501.
28. K. Zagorodniy, M. Taut and H. Herman, *Phys. Rev. A*, 2006, **73**, 054501.
29. A. N. Vereshchagin, *Polarizability of Molecules*, Nauka: Moscow, 1980.
30. A. D. Buckingham, *Adv. Chem. Phys.*, 1967, **12**, 107.
31. S. Gerlich, L. Hackermüller, A. Stibor, H. Ulbricht, F. Goldfarb, T. Savas, M. Müri, M. Mayor and M. Arndt, *Nature Phys.*, 2007, *3*, 711.
32. S. Gerlich, S. Eibenberger, M. Tomandl, S. Nimmrichter, K. Hornberger, P. J. Fagan, J. Tüxen, M. Mayor and M. Arndt, *Nature Commun.*, 2011, **2**, 263.

33. J. E. Gready, G. B. Bacskay and N. S. Hush, *Chem. Phys.*, 1977, **24**, 333.
34. B. Shanker and J. Applequist, *J. Phys. Chem.*, 1994, **98**, 6486.
35. D. Fuchs, H. Rietschel, R. H. Michel, A. Fischer, P. Weis, and M. M. Kappes, *J. Phys. Chem.*, 1996, **100**, 725.
36. D. Jonsson, P. Norman, K. Ruud, H. Ågren and T. Helgaker, *J. Chem. Phys.*, 1998, **109**, 572.
37. A. Ballard, K. Bonin and J. Louderback, *J. Chem. Phys.*, 2000, **113**, 5732.
38. I. Compagnon, R. Antoine, M. Broyer, Ph. Dugourd, J. Lermé and D. Rayane, *Phys. Rev. A*, 2001, **64**, 025201.
39. A. V. Luzanov, A. D. Bochevarov and O. V. Shishkin, *J. Struct. Chem.*, 2001, **42**, 296.
40. L. Jensen, P.-O. Åstrand and K. V. Mikkelsen, *J. Phys. Chem. B*, 2004, **108**, 8226.
41. Y. H. Hu and E.Ruckenstein, *J. Chem. Phys,* 2005, **123**, 214708.
42. M. Berninger, A. Stefanov, S. Deachapunya and M. Arndt, *Phys. Rev. A*, 2007, **76**, 013607.
43. R. R. Zope, *J. Phys. B: At. Mol. Opt. Phys.*, 2007, **40**, 3491.
44. R. G. Bulgakov, D. I. Galimov and D. Sh. Sabirov, *JETP Lett.*, 2007, **85**, 632.
45. D. Sh. Sabirov, S. L. Khursan and R. G. Bulgakov, *J. Mol. Graph. Model.*, 2008, **27**, 124.
46. R. R. Zope, T. Baruah, M. R. Pederson and B. I. Dunlap, *Phys. Rev. B*, 2008, **77**, 115452.
47. A. Alparone, V. Librando and Z. Minniti, *Chem. Phys. Lett.*, 2008, **460**, 151.
48. R. R. Zope, *J. Phys. B: At. Mol. Opt. Phys.*, 2008, **41**, 085101.
49. D. Martin, S. Sild, U. Maran and M. Karelson, *J. Phys. Chem. C*, 2008, **112**, 4785.
50. D. Sh. Sabirov, S. L. Khursan, R. G. Bulgakov and U. M. Dzhemilev, *Dokl. Phys. Chem.*, 2009, **425**, 54.
51. D. Rappoport and F. Furche, *J. Chem. Phys.*, 2010, **133**, 134105.
52. P. Calaminici, J. Carmona-Espindola, G. Geudtner and A. M. Köster, *Int. J. Quantum Chem.*, 2012, **112**, 3252.
53. D. Sh. Sabirov, R. R. Garipova and R. G. Bulgakov, *Chem. Phys. Lett.*, 2012, **523**, 92.
54. F. E. Jorge, M. K. Morigaki and S. S. Jorge, *Ind. J. Chem.*, 2012, **51A**, 911.
55. A. V. Marenich, C. J. Cramer and D. G. Truhlar, *Chem. Sci.*, 2013, **4**, 2349.
56. A. Peyghan, H. Soleymanabadi and M. Moradi, *J. Phys. Chem. Solids*, 2013, **74**, 1594.
57. D. Sh. Sabirov, A. O. Terentyev, I. S Shepelevich and R. G. Bulgakov, *Comput. Theor. Chem.*, 2014, **1045**, 86.
58. V .A. Maltsev, O. A. Nerushev, S. A. Novopashin, and B. A. Selivanov, *JETP Lett.*, 1993, **57**, 653.
59. V .A. Maltsev, O. A. Nerushev and S. A. Novopashin, *Chem. Phys. Lett.*, 1993, **212**, 480.
60. B. Bernardo, D. Cheyns, B. Verreet, R.D. Schaller, B.P. Rand and N.C. Giebink, *Nat. Commun.*, 2014, **5**, 3245.
61. D. Sh. Sabirov, A. O. Terentyev and R. G. Bulgakov, *Phys. Chem. Chem. Phys.*, 2014, **16**, 14594.
62. A. F. Shestakov, *Russ. J. Gen. Chem.*, 2008, **78**, 811.
63. D. Sh. Sabirov and R. G. Bulgakov, *Comput. Theor. Chem.*, 2011, **963**, 185.
64. E. Yu. Pankratyev, A. R. Tulyabaev and L. M. Khalilov, *J. Comput. Chem.*, 2011, 32, 1993.
65. L. M. Khalilov, A. R. Tulyabaev, V. M. Yanybin and A. R. Tuktarov, *Magn. Reson. Chem.*, 2011, **49**, 378.
66. B. Champagne, E. A. Perpète and J.-M. André, *J. Chem. Phys.*, 1994, **101**, 10796.
67. C. D. Zeinalipour-Yazdi and D. P. Pullman, *J. Phys. Chem. B*, 2008, **112**, 7377.
68. D. Sh. Sabirov, *Comput. Theor. Chem.*, 2014, **1030**, 81.
69. J. F. Ye, H. Chen, R. Note, H. Mizuseki and Y. Kawazoe, *J. Phys. Org. Chem.*, 2008, **21**, 789.
70. P. Karamanis, C. Pouchan and g. Maroulis, *Phys. Rev. A*, 2008, **77**, 013201.
71. L. Jensen, P.-O. Åstrand and K. V. Mikkelsen, *J. Phys. Chem. A*, 2004, **108**, 8795.
72. A. Kumar and A. J. Thakkar, C*hem. Phys. Lett.*, 2011, **516**, 208.
73. V. N. Bezmel'nitsyn, A. V. Eletskii and M. V. Okun', *Phys. Usp.*, 1998, **41**, 1091.
74. D. V. Konarev and R. N. Lyubovskaya, *Russ. Chem. Rev.*, 1999, **68**, 19.
75. S. H. Patil, K. D. Sen and V. P. Varshni, *Can. J. Phys.*, 2005, **83**, 919.
76. M. Ya. Amusia, L. V. Chernysheva and E. Z. Liverts, *Phys. Rev. A*, 2009, **80**, 032503.
77. V. L. Ermolaev, E. N. Bodunov, E. B. Sveshnikova and T. A. Shakhverdov, *Nonradiative Transfer of Electron Excitation Energy*, Nauka: Leningrad, 1977.
78. Z. Z. Latypov and O. F. Pozdnyakov, *Techn. Phys. Lett.*, 2006, **32**, 381.
79. D. Sh. Sabirov, R. G. Bulgakov and S. L. Khursan, *ARKIVOC*, 2011(8), 200.
80. S. Bhattacharya, S. K. Nayak, S. Chattopadhyay, M. Banerjee and A. K. Mukherjee, *J. Phys. Chem. A*, 2001, **105**, 9865.
81. E. D. Davis, A. Wagner, M. McEntee, M. Kaur, D. Troya and J. R. Morris, *J. Phys. Chem. Lett.*, 2012, **3**, 3193.
82. R. C. Chapleski, J. R. Morris and D. Troya, *Phys. Chem. Chem. Phys.*, 2014, **16**, 5977.
83. D. Sh. Sabirov, S. L. Khursan and R. G. Bulgakov, *Vestn. Bashkir. Univ.*, 2007, **12**(2), 18.
84. A. N. Turanov and Kremenskaya, *Russ. Chem. Bull.*, 1994, **43**, 240.
85. L. I. Buravov, O. A. D'yachenko, S. V. Konovalikhin, N. D. Kushch, I. P. Lavrent'ev, N. G. Spitsyna, G. V. Shilov and E. B. Yagubskii, *Russ. Chem. Bull.*, 1994, **43**, 240.
86. D. Sh. Sabirov, *PhD Thesis*, Bashkir State University, 2009, Ufa, Russia.
87. D. Heymann and R. B. Weisman, *C. R. Chimie*, 2006, **9**, 1107.
88. R. G. Bulgakov, D. Sh. Sabirov and U. M. Dzhemilev, *Russ. Chem. Bull.*, 2013, **62**, 304.
89. C. Thilgen and F. Diederich, *Chem. Rev.*, 2006, ***106***, 5049.
90. R. B. Weisman, S. M. Bachilo and D. Heymann, *J. Amer. Chem. Soc.*, 2002, **124**, 6317.
91. M. L. Kuznetsov, *Russ. Chem. Rev.*, 2006, **75**, 935.
92. D. Sh. Sabirov and R. G. Bulgakov, *Fullerene Nanotube Carbon Nanostruct.*, 2010, **18**, 455.
93. D. Sh. Sabirov, S. L. Khursan and R. G. Bulgakov, *Vestn. Bashkir. Univ.*, 2008, **13**, 764.

94. X. Lu, F. Tian, X. Xu, N. Wang and Q. Zhang, *J. Am. Chem. Soc.*, 2003, **125**, 10459
95. Z. Chen, W. Thiel and A. Hirsch, Chem. Phys. Chem., 2003, **4**, 93.
96. D. Sh. Sabirov, S. L. Khursan and R. G. Bulgakov, *Russ. Chem. Bull.*, 2008, **57**, 2520.
97. Z. Xiao, F. Wang, S. Huang, L. Gan, J. Zhou, G. Yuan, M. Lu and J. Pan, *J. Org. Chem.*, 2005, **70**, 2060.
98. B. Li, C. Shu, X. Lu, L. Dunsch, Z. Chen, T. J. S. Dennis, Z. Shi, L. Jiang, T. Wang, W. Xu and C. Wang, *Angew. Chem.*, 2010, **49**, 962.
99. R. R. Zope and T. Baruah, *Phys. Rev. B*, 2009, **80**, 033410.
100. O. V. Sedel'nikova, L. G. Bulusheva and A. V. Okotrub, *Phys. Solid State*, 2009, **51**, 863.
101. J. Jiang, J. Dong and D. Y. Xing, *Solid State Commun.*, 1997, **101**, 537.
102. L. X. Benedict, S. G. Louie and M. L. Cohen, *Phys. Rev. B*, 1995, **52**, 8541.
103. E. N. Brothers, A. F. Izmaylov, G. E. Scuseria and K. N. Kudin, *J. Phys. Chem. C*, 2008, **112**, 1396.
104. L. Jensen, P.-O. Åstrand and K. V. Mikkelsen, *Nano Lett.*, 2003, **3**, 8451.
105. J. Kongsted, A. Osted, L. Jensen, P.-O. Åstrand and K. V. Mikkelsen, *J. Phys. Chem. B*, 2001, **105**, 10243.
106. M. Z. Kassaee and H. A. Rad, *Comput. Mater. Sci.*, 2010, **48**, 144.
107. A. Mohajeri and A. Omidvar, *J. Phys. Chem. C*, 2014, **118**, 1739.
108. D. Ugarte, A. Châtelain and W. A. de Heer, *Science*, 1996, **274**, 1897.
109. D. Ugarte, T. Stöckli, J. M. Bonard, A. Châtelain and W. A. de Heer, *Appl. Phys.*, 1998, **67**, 101.
110. P. G. de Gennes, *Rev. Mod. Phys.*, 1985, **57**, 827.
111. M. R. Pederson and J. Q. Broughton, *Phys. Rev. Lett.*, 1992, **69**, 2689.
112. M. R. Pederson, A. A. Quong, J. Q. Broughton and J. L. Feldman, *Comput. Mater. Sci.*, 1994, **2**, 536.
113. M. D. Halls and H. B. Schlegel, *J. Phys. Chem. B*, 2002, **106**, 1921.
114. M. D. Halls and K. Raghavachari, *Nano Lett.*, 2005, **5**, 1861.
115. A. V. Tazylin, I. V. Anoshkin, A. V. Krasheninnikov, R. M. Nieminen, A. G. Nasibullin, H. Jiang and E. I. Kauppinen, *Nano Lett.*, 2011, **11**, 4352.
116. X. Pan and X. Bao, *Acc. Chem. Res.*, 2011, **44**, 553.
117. R. Ravinder and V. Subramanian, *J. Phys. Chem. C*, 2013, **117**, 5095.
118. P. Giacinto, A. Bottoni, M. Calvaresi and F. Zerbetto, *J. Phys. Chem C*, 2014, **118**, 5032.
119. V. Barone, M. Cossi and J. Tomasi, *J. Comp. Chem.*, 1998, **19**, 404.
120. M. Murata, Y. Murata and K. Komatsu, *Chem. Commun.*, 2008, 6083.
121. C. M. Stanisky, R. J. Cross and M. Saunders, *J. Am. Chem. Soc.*, 2009, **131**, 3392.
122. L. Gan, D. Yang, Q. Zhang and H. Huang, *Adv. Mater.*, 2010, **22**, 1498.
123. Y. H. Hu and E.Ruckenstein, *J. Am. Chem. Soc.,* 2005, **127**, 11277.
124. Y. Yang, F.-H. Wang and Y.-S. Zhou, *Phys. Rev. A,* 2005, **71**, 013202.
125. C. R. Zhang, W. Z. Liang, H. S. Chen, Y. H. Chen, Z. Q. Wei and Y. Z. Wu, *J. Mol. Struct. THEOCHEM*, 2008, **862**, 98.
126. C. R. Zhang, H. S. Chen, Y. H. Chen, Z. Q. Wei and Z. S. Pu, *Acta Phys. Chim. Sin. (Wuli Huaxue Xuebao),* 2008, **24**, 1353.
127. R. Rivelino, T. Malaspina and E. E. Fileti, *Phys. Rev. A*, 2009, **79**, 013201.
128. S.-W. Tang, J.-D. Feng, Y.-Q. Qiu, H. Sun, F.-D. Wang, Y.-F. Chang and R.-S. Wang, *J. Comput. Chem.*, 2010, **31**, 2650.
129. C. Tang, W. Zhu and K. Deng, *Chin. J. Chem.*, 2010, **28**, 1355.
130. S.-W. Tang, J.-D. Feng, Y.-Q. Qiu, H. Sun, F.-D. Wang, Z.-M. Su, Y.-F. Chang and R.-S. Wang, *J. Comput. Chem.*, 2011, **32**, 658.
131. D. Sh. Sabirov and R. G. Bulgakov, *Chem. Phys. Lett.*, 2011, **506**, 52.
132. D. Sh. Sabirov, A. A. Tukhbatullina and R. G. Bulgakov, *Comput. Theoret. Chem.*, 2012, **993**, 113.
133. D. Sh. Sabirov, R. R. Garipova and R. G. Bulgakov, *Fullerenes Nanotubes Carbon Nanostruct.*, 2012, **20**, 386–390.
134. C.Tang, W. Zhu, H. Zou, A. Zhang, J. Gong and C. Tao, *Comput. Theor. Chem.*, 2012, **991**, 154.
135. D. Sh. Sabirov, *J. Phys. Chem. C*, 2013, **117**, 9148.
136. C.-R. Zhang, L.-H. Han, J.-W. Zhe, N.-Z. Jin, Y.-L. Shen, L.-H. Yuan, Y.-Z. Wu and Z.-J. Liu, *J. Nanomaterials*, 2013, 612153.
137. K. Akhtari, K. Hassanzadeh, B. Fakhraei, H. Hassanzadeh, G. Akhtari and S. A. Zarei, *Comput. Theor. Chem.*, 2014, **1038**, 1.
138. K. Hornberger, S. Gerlich, H. Ulbricht, L. Hackermüller, S. Nimmrichter, I. V. Goldt, O. Boltalina and M. Arndt, *New J. Phys.*, 2009, **11**, 043032.
139. B. W. Larson, J. B. Whitaker, A. A. Popov, N. Kopidakis, G. Rumbles, O. V. Boltalina and S. H. Strauss, *Chem. Mater.*, 2014, **26**, 2361.
140. M. V. Reinov and M. A. Yurovskaya, *Russ. Chem. Rev.*, 2007, **76**, 715.
141. N. P. Curry, B. Doust and D. A. Jelski, *J. Cluster Sci.*, 2000, **12**, 385.
142. I. Lamparth and A. Hirsch, *J. Chem. Soc. Chem. Commun.*, 1994, 1727.
143. D. J. Wolff, C. M. Barbieri, C. F. Richardson, D. I. Schuster and S. R. Wilson, *Arch. Biochem. Biophys.*, 2002, **399**, 130.
144. B. Sitharaman, S. Asokan, I. Rusakova, M. S. Wong and L. J. Wilson, *Nano Lett.*, 2004, **4**, 1759.
145. A. G. Avent and R. Taylor, *Chem. Commun.,* 2002, 2726.
146. S. M. Avdoshenko, I. N. Ioffe, and L. N. Sidorov, *J. Phys. Chem. A,* 2009, **113**, 10833.
147. A. J. Thakkar, *AIP Conf. Proc.*, 2012, **1504**, 586.
148. O. Zhou and D. E. Cox, *J. Phys. Chem. Solids*, 1992, **53**, 1373.
149. U. M. Dzhemilev, A. R. Tuktarov, I. R. Yarullin and A. R. Akhmetov, *Mendeleev Commun.*, 2013, **23**, 326.
150. X.-Y. Ren and Z.-Y. Liu, *J. Mol. Graph. Model*., 2007, **26**, 336.
151. T. Umeyama and H. Imahori, *J. Mater. Chem*., 2014, **2**, 11545.
152. S. Kitaura, K. Kurotobi, M. Sato, Y. Takano, T. Umeyama and H. Imahori, C*hem. Commun.*, 2012, **48**, 8550.
153. D. Scanu, N. P. Yevlampieva, R. Deschenaux, *Macromolecules,* 2007, **40**, 1133.
154. M. Frost, M. A. Faist and J. Nelson, *Adv. Mater.*, 2010, *22*, 4881.
155. X. Meng, G. Zhao, Q. Xu, Z. Tan, Z. Zhang, L. Jiang, C. Shu, C. Wang and Y. Li, *Adv. Funct. Mater.*, 2014, **24**, 158.
156. L. J. A. Koster, S. E. Shaheen and J. C. Hummelen, *Adv. Energy Mat.*, 2012, **2**, 1246.

157. K.-H. Kim, H. Kang, H. J. Kim, P. S. Kim, S. C. Yoon and B. J. Kim, *Chem. Mater.*, 2012, **24**, 2373.
158. M. Lenes, S. W. Shelton, A. B. Sieval, D. F. Kronholm, J. C. Hummelen and P. W. M. Blom, *Adv. Funct. Mater.*, 2009, **19**, 3002.
159. C. Dyer-Smith, L. X. Reynolds, A. Bruno, D. D. C. Bradley, S. A. Haque and J. Nelson, *Adv. Funct. Mater.*, 2010, *20*, 2701.
160. C.-Z. Li, H.-L. Yip and A. K.-Y. Jen, *J. Mater. Chem.*, 2012, **22**, 4161.
161. J. C. Hummelen, B. W. Knight, F. Le Peq, F. Wudl, J. Yao and C. L. Wilkins, *J. Org. Chem.*, 1995, **60**, 532.
162. M. M. Wienk, J. M. Kroon, W. J. H. Verhees, J. Knol, J. C. Hummelen, P. A. van Hal and R. A. J. Janssen, *Angew. Chem.*, 2003, **115**, 3493.
163. J. L. Segura and N. Martin, *Chem. Soc. Rev.*, 2000, **29**, 13.
164. L. Zhechkov, T. Heine and G. Seifert, *J. Phys. Chem. A*, 2004, **108**, 11733.
165. D. Sh. Sabirov, *RSC Adv.*, 2013, **3**, 19430.
166. Y. Shirai, A. J. Osgood, Y. Zhao, K. F. Kelly and J. M. Tour, *Nano Lett*., 2005, **5**, 2330.
167. S. Lu, T. Jin, M. Bao and Y. Yamamoto, *Org. Lett.*, 2012, **14**, 3466.
168. S. Ōsawa, M. Sakai and E. Ōsawa, *J. Phys. Chem. A*, 1997, 101, 1378.
169. K. Komatsu, G.-W. Wang, Y. Murata, T. Tanaka and K. Fujiwara, *J. Org. Chem.*, 1998, **63**, 9358.
170. M. Kunitake, S. Uemura, O. Ito, K. Fujiwara, Y. Murata and K. Komatsu, *Angew. Chem.*, 2002, **114**, 1011.
171. R. W. Munn and P. Petelenz, *Chem. Phys. Lett.*, 2004, **392**, 7.
172. S. Hati and D. Datta, *J. Phys. Chem.*, 1994, **98**, 10451.
173. T. K. Ghanty and S. K. Ghosh, *J. Phys. Chem.*, 1996, **100**, 12295
174. U. Holm, *J. Phys. Chem. A*, **2000**, 104, 8418
175. S. A. Blair and A. J. Thakkar, C*hem. Phys. Lett.*, 2013, **556**, 346.
176. K. Fujiwara and K. Komatsu, *Chem. Commun.*, 2001, 1986.
177. A. A. Goryunkov, I. N. Ioffe, P. A. Khavrel, S. M. Avdoshenko, V. Yu. Markov, Z. Mazej, L. N. Sidorov and S. I. Troyanov, *Chem. Commun.*, 2007, 704.
178. D. Sun and C. A. Reed, *Chem. Commun.*, 2000, 2391.
179. D. Sh. Sabirov, R. R. Garipova and R. G. Bulgakov, *J. Phys. Chem. A*, 2013, **117**, 13176.
180. H. Tian and S. Yang, *Chem. Soc. Rev.*, 2004, **33**, 85169.
181. A. Mateo-Alonso, D. M. Guldi, F. Paolucci and M. Prato, *Angew. Chem. Int. Ed.*, 2007, **46**, 8120.
182. H. Sasabe and T. Takata, *J. Porphyrins Phthalocyanines*, 2007, **11**, 334.
183. S. Minikata, R. Tsuruoka, T. Nagamachi, and M. Komatsu, *Chem. Commun.*, 2008, 323.
184. J. Zhang, K. Porfyrakis, J. J. L. Morton, , M. R. Sambrook, J. Harmer, L. Xiao, A. Ardavan and G. A. D. Briggs, *J. Phys. Chem. C*, 2008, **112**, 2802.
185. C. M. Isborn, C. Tang, A. Martini, E. R. Johnson, A. Otero-de-la-Roza and V. C. Tung, *J. Phys. Chem. Lett.,* 2013, **4**, 2914.
186. M. D. Tzirakis and M. Orfanopoulos, *Chem. Rev.*, 2013, **113**, 5262.
187. Y.-K. Zhang, E. G. Janzen and Y. J. Kotake, *Chem. Soc. Perkin Trans. 2*, 1996, 1191.
188. R. G. Bulgakov, Yu. G. Ponomareva and R. A. Sadykov, *Russ. Chem. Bull.,* 2008, **57**, 2028.
189. Y. Abe, H. Tanaka, Y. Guo, Y. Matsuo and E. Nakamura, *J. Amer. Chem. Soc.*, 2014, **136**, 3366.
190. L. Zoppi, K. K. Baldridge, A. Ferretti, *J. Chem. Theory Comput.*, 2013, **9**, 4797.
191. S. Liu and S. Sun, *J. Organomet. Chem.*, 2000, **599**, 74.
192. S. Guha and K. Nakamoto, *Coord. Chem. Rev.*, 2005, **249**, 1111.
193. X. Lu, L. Feng, T. Akasaka and S. Nagase, *Chem. Soc. Rev.*, 2012, **41**, 7723.
194. A. A. Popov, S. Yang and L. Dunsch, *Chem. Rev.*, 2013, **113**, 5989.
195. S. Osuna, M. Swart and M. Solà, *Chem. Eur. J.*, 2009, **15**, 13111.
196. S. Osuna, M. Swart and M. Solà, *Phys. Chem. Chem. Phys.*, 2011, **13**, 3585.
197. A. Vlandas, C. P. Ewels and G. van Lier, *Chem. Commun.*, 2011, **47**, 7051.
198. A. L. Buchachenko, *J. Phys. Chem. B,* 2001, **105***,* 5839.
199. F. Torrens, *Microelectron. Eng.*, 2000, **51–52**, 613.
200. F. Torrens, *Nanotechnology*, 2002, **13**, 433.
201. F. Torrens, *J. Phys. Org. Chem.*, 2002, **15**, 742.
202. R. Langlet, A. Mayer, N. Geuquet, H. Amara, M. Vandescuren, L. Henrard, S. Maksimenko and P. Lambin, *Diamond Relat. Mater.*, 2007, **16**, 2145.
203. R. Langlet, P. Lambin, A. Mayer, P. P. Kuzhir and S. A. Maksimenko, *Nanotechnology*, 2008*,* **19**, 115706.
204. F. Moreau, R. Langlet, P. Lambin, P. P. Kuzhir, D. S. Bychanok and S. A. Maksimenko, *Solid State Sci.*, 2009, **11**, 1752.
205. H. Yan, S. Yu, X. Wang, Y. He, W. Huang and M. Yang, *Chem. Phys. Lett.*, 2008, **456**, 223.
206. D. Sh. Sabirov and R. G. Bulgakov, *JETP Lett.,* 2010, **92**, 662.
207. D. Sh. Sabirov, E. S. Malinov, I. S. Shepelevich and R. G. Bulgakov, *Vestn. Bashkir. Univ.*, 2010, **15**, 1127.
208. D. Sh. Sabirov, R. R. Garipova, A. R. Khasanov and R. G. Bulgakov, *Vestn. Bashkir. Univ.*, 2011, **16**, 16.
209. D. Sh. Sabirov, *J. Phys. Chem. C*, 2013, **117**, 1178.
210. K. Jackson, M. Yang and J. Jellinek, *J. Phys. Chem. C*, 2013, **111**, 17952.
211. P. Delaney and J. C. Greer, *Appl. Phys. Lett.*, 2004, **84**, 431.
212. D. Sh. Sabirov, A. O. Terentyev and R. G. Bulgakov, *Vestn. Bashkir. Univ.*, 2013, **18**, 1006.
213. Y. Morinaka, S. Sato, A. Wakamiya, H. Nikawa, N. Mizorogi, F. Tanabe, M. Murata, K. Komatsu, K. Furukawa, T. Kato, S. Nagase, T. Akasaka, Y. Murata, *Nature Commun.*, 2013, **4**, 1554.
214. A. Galano, A. Pérez-González, L. del Olmo, M. Francisco-Marquez and J. R. Léon-Carmona, *J. Mol. Model.*, 2014, **20**, 2412.
215. C. Meyer, W. Harneit, B. Naydenov, K. Lips and A. Weidinger, *Appl. Magnet. Reson.*, 2004, **27**, 123.
216. S. C. Benjamin, A. Ardavan, G. A. D. Briggs, D. A. Britz, D. Gunlycke, J. Jefferson, M. A. G. Jones, D. F. Leigh, B. W. Lovett, A. N. Khlobystov, S. A. Lyon, J. J. L. Morton, K. Porfyrakis, M. R. Sambrook and A. M. Tyryshkin, *J. Phys.: Condens. Matter,* 2006, **18**, S867.
217. J. J. L. Morton, A. M. Tyryshkin, A. Ardavan, S. C. Benjamin, K. Porfyrakis, S. A. Lyon and G. A. D. Briggs, *Phys. Stat. Sol. B*, 2006, **243**, 3028.
218. L. Tsetseris, *J. Phys. Chem. C*, 2011, **115**, 3528.
219. M. I. A. Oliveira, R. Rivelino, F. de Brito Mota and G. K. Gueorguiev, *J. Phys. Chem. C*, 2014, **118**, 5501.

220. S. G. Semenov and M. E. Bedrina, *J. Struct. Chem.*, 2013, **54**, 159.
221. X. Fan, L. Xu, L. Liu, M. Yang, Q. Zeng and M. Yang, *Comput. Theor. Chem.*, 2013, **1013**, 52.
222. H. Reis, O. Loboda, A. Avramopoulos, M. G. Papadopoulos, B. Kirtman, J. M. Luis and R. Zaleśky, *J. Comput. Chem.*, 2011, **32**, 908.
223. B. Skwara, R. W. Góra, R. Zaleśny, P. Lipkowski, W. Bartkowiak, H. Reis, M. G. Papadopoulos, J. M. Luis and B. Kirtman, *J. Phys. Chem. A*, 2011, **115**, 10370.
224. J. He, K. Wu, R. Sa, Q. Li and Y. Wei, *Chem. Phys. Lett.*, 2009, **475**, 73.
225. L. Xu, H. Tang, C. Li, F. Li, X. Li and S. Tao, *Struct. Chem.*, 2013, **24**, 463.
226. C. Tang, S. Fu, K. Deng, Y. Yuan, W. Tan, D. Huang and X. Wang, *J. Mol. Struct. THEOCHEM*, 2008, **867**, 111.
227. C. Tang, W. Zhu and K. Deng, *J. Mol. Struct. THEOCHEM*, 2009, **894**, 112.
228. H. Lamparczyk, D. Wilczyńska and A. Radecki, *Chromatographia*, 1981, **14**, 707.
229. C.-M. Tang, Q.-S. Cao, W.-H. Zhu and K. M. Deng, *Chin. Phys. B*, 2010, **19**, 033603.
230. S. A. Ndengué and O Motapon, *J. Phys. B: At. Mol. Opt. Phys.*, 2008, 41, 045001.
231. O. Motapon, S. A. Ndengue and K. D. Sen, Int. J. Quantum Chem., 2011, 111, 4425.
232. C. A. Reed and R. D. Bolskar, *Chem. Rev.*, 2000, **100**, 1075.
233. D. Sh. Sabirov, A. D. Zakirova, A. A. Tukhbatullina, I. M. Gubaydullin and R. G. Bulgakov, *RSC Adv.*, 2013, **3**, 1818.
234. S. M. Smith, A. N. Markevitch, D. A. Romanov, X. Li, R. J. Levis and H. B. Schlegel, *J. Phys. Chem. A*, 2004, **108**, 11063.
235. M. Broyer, R. Antoine, I. Compagnon, D. Rayane and Ph. Dugourd, *Phys. Scr.*, 2007, **76**, C135.
236. R. Antoine, D. Rayane, Ph. Dugourd, E. Benichou and M. Broyer, *Eur. Phys. J. D*, 2000, **12**, 147.
237. D. Rayane, R. Antoine, Ph. Dugourd, E. Benichou, A. R. Allouche, M. Aubert-Frécon and M. Broyer, *Phys. Rev. Lett.*, 2000, **84**, 1962.
238. F. Rabilloud, R. Antoine, M. Broyer, I. Compagnon, Ph. Dugourd, D. Rayane, F. Calvo and F. Spiegelman, *J. Phys. Chem. C*, 2007, **111**, 17795.
239. Y.-F. Wang, Y. Li, Z.-R. Li, F. Ma, D. Wu and C.-C. Sun, *Theor. Chem. Acc.*, 2010, **127**, 641.
240. R. Anderson and A. R. Barron, *J. Am. Chem. Soc.*, 2005, **127**, 10458.
241. R. Macovez, M. Zachariah, M. Romanini, P. Zygouri, D. Gournis, and J. L. Tamarit, *J. Phys. Chem. C*, 2014, **118**, 12170.
242. J. R. Danielson, J. A. Young, C. M. Surko, *J. Phys. B: At. Mol. Opt. Phys.*, 2009, **42**, 235203.
243. A. D. Chepelianskii, J. Wang and R. H. Friend, *Phys. Rev. Lett.*, 2014, **112**, 126802.
244. A. S. Shalabi, M. M. Assem, S. A. Aal, W. S. A. Halim and E. A. M. Mahdy, *Quant. Matter*, 2014, **3**, 29.
245. H. M. Ahmed, M. K. Hassan, K. A. Mauritz, S. L. Bunkley, R. K. Buchanan and J. P. Buchanan, *J. Appl. Polym. Sci.*, 2012, **131**, 40577.
246. C. A. Jimenez-Cruz, S. Kang and R. Zhou, *WIREs Syst. Biol. Med.*, 2014, **6**, 329.
247. R. Meir, H. Chen, W. Lai and S. Shaik, *ChemPhysChem*, 2010, **11**, 301.
248. H. Beg, S. P. De, S. Ash and A. Misra, *Comput. Theor. Chem.*, 2012, **984**, 13.
249. A. Roztoczyńska, J. Kozłowska, P. Lipkowski and W. Bartkowiak, *Chem. Phys. Lett.*, 2014, **608**, 264.
250. F. Torrens, *Nanotechnology*, 2004, **15**, S259.
251. Y. J. Dappe, *J. Phys. D: Appl. Phys.*, 2014, **47**, 083001.
252. M. V. Suyetin and A. V. Vakhrushev, *Nanoscale Res. Lett.*, 2009, **4**, 1267.
253. J. Zhou, Q. Wang, Q. Sun, P. Jena and X. S. Chen, *Proc. Nat. Acad. Sci.*, 2010, **16**, 2801.
254. M. V. Suyetin and A. V. Vakhrushev, *J. Phys. Chem. C*, 2011, **115**, 5485.
255. D. Herschbach, *Rev. Mod. Phys.*, 1999, **71**, S411.
256. E. Gershnabel and I. Sh. Averbukh, *Phys. Rev. Lett.*, 2010, **104**, 153001.
257. A. V. Akimov and A. B. Kolomeisky, *J. Phys. Chem. C*, 2012, **116**, 22595.

Denis Sh. Sabirov was born in 1984 in Magnitogorsk (Russia). In 2009, he received his PhD in the fields of physical, mathematical, and quantum chemistry in Bashkir State University (Ufa, Russia). Currently, he is a senior researcher in the Institute of Petrochemistry and Catalysis of Russian Academy of Sciences. His current interests involve applications of DFT to chemical and physical processes in carbon nanostructures with focus on their polarizability.

